REPUBLIC OF TÜRKİYE
KARADENIZ TECHNICAL UNIVERSITY
GRADUATE SCHOOL OF HEALTH SCIENCES

DEPARTMENT OF PHYSIOLOGY

IRON AND UTERINE CONTRACTION: AN EXPERIMENTAL INVESTIGATION OF THE EFFECT OF IRON DEFICIENCY ANEMIA ON MYOMETRIAL CONTRACTION

Mahindokht ROUHIKIA

DOCTORAL THESIS

Prof. Dr. Ahmet AYAR

TRABZON-2025

THESIS ETHIC DECLARATION

I hereby declare that this thesis has been conducted and written in accordance with the standards of the Thesis Preparation and Writing Guide of the Institute of Health Sciences at Karadeniz Technical University; that it is an original scientific research work carried out in compliance with academic and ethical principles; that all information and interpretations not obtained through this study have been duly cited, and the sources used are listed in the references section; and that no act violating patent or copyright laws has been committed during the research and writing stages of this thesis.

18.09.2025
Mahindokht ROUHIKIA
(İmza)

Dedication

To all those born with complications associated with maternal anemia, who strive each day to live and to thrive, this thesis is dedicated to you.

ACKNOWLEDGMENTS

First and foremost, all praise and gratitude are due to Allah, the Almighty, for His boundless mercy, guidance, and strength throughout the course of this thesis.

It has been a true privilege to pursue this academic journey under the supervision of Prof. Dr. Ahmet Ayar, whose profound insight, patient mentorship, and unwavering encouragement laid the foundation for my academic development, and whose timely guidance at critical moments was instrumental in shaping the direction of this thesis.

I am equally grateful to Prof. Dr. Sibel Velioğlu and Prof. Dr. Ali Osman Kılıç, whose invaluable feedback as jury members enriched the quality and rigor of this work.

My sincere thanks also extend to Prof. Mukadder Okuyan, whose enduring friendship and steadfast support were a source of strength throughout this journey. In addition, I warmly thank Research Assistant Burak Özgören, and my peers in the Department of Physiology for their support.

Above all, my most profound thanks belong to my beloved family. To my husband, Dr. Nasrollah Mostofi, your resolute love and unwavering belief in me have carried me through every challenge. At every step, you stood by me, offering strength in silence and encouragement in hardship. This achievement would not have been possible without you.

To my daughters, Fatemeh, Sara, and Laya, your joy, laughter, and unshakable love turned the most difficult days into bearable ones and gave me the courage to press forward. Pursuing this journey at Karadeniz Technical University alongside you has been the greatest privilege of my life. You have been my source of energy, wisdom, and emotional grounding throughout this journey. You are not only the heartbeat of my life, you are the most beautiful thesis I have ever written.

In loving memory of my parents, Moloud Malek Shoar and Reza Rouh, whose legacy of love and learning lives on through this work.

Mahindokht Rouhikia

CONTENTS

LIST OF TABLES

LIST OF FIGURES

LIST OF ABBREVIATIONS, SYMBOLS, AND FORMULAS

ABBREVIATIONS

AP	Aksiyon Potansiyeli (Action Potential)
A.S.P	Adrenal Spesifik Protein
ATP	Adenozin Trifosfat (Adenosine Triphosphate)
AUC	Eğri Altındaki Alan (Area Under the Curve)
BSL	BIOPAC Student Lab (Analiz sistemi/yazılımı)
CI	Güven Aralığı (Confidence Interval)
EDTA	Etilendiamintetraasetik Asit (Ethylenediaminetetraacetic Acid)
GD	Gebelik Günü (Gestational Day)
Hb	Hemoglobin
Hct	Hematokrit
IDA	Demir Eksikliği Anemisi (Iron Deficiency Anemia)
i.p.	İntraperitoneal
IV	İntravenöz (Intravenous)
KATP	ATP-duyarlı Potasyum Kanalı (ATP-sensitive Potassium Channel)
KH	Krebs–Henseleit (tampon/çözelti)
KTÜ	Karadeniz Teknik Üniversitesi
MSMCs	Myometriyal Düz Kas Hücreleri (Myometrial Smooth Muscle Cells)
OR	Olasılık Oranı (Odds Ratio)
RH	Bağıl Nem (Relative Humidity)
RMP	Dinlenim Zar Potansiyeli (Resting Membrane Potential)
SERCA	Sarkoplazmik/Endoplazmik Retikulum Ca^{2+}-ATPazı
SLO2.1	Sodyumla Aktive K^+ Kanalı (SLO2.1)
TÜBİTAK	Türkiye Bilimsel ve Teknik Araştırma Kurumu

ÖZET

Demir ve Uterus Kasılması: Demir Eksikliği Anemisinin Miyometriyum Kasılması Üzerine Etkisine Yönelik Deneysel Bir İnceleme

Demir eksikliği anemisi (DEA) gebelikte en sık görülen beslenme bozukluklarından biridir ve anne-fetal sonuçları olumsuz etkiler. Ancak DEA'nın gebeliğin son döneminde miyometriyumun pasif tonu ve kendiliğinden kasılma dinamikleri üzerindeki doğrudan etkisi yeterince nicel olarak ortaya konmamıştır.. Mevcut literatür aktif kasılma yanıtlarına odaklanırken, DEA'nın pasif rahim tonusu ve ritmik faz kasılma işine (AUC) etkisini, (başlangıç stres-relaksasyon dönemi dışlanarak ve dengeye ulaşıldıktan sonra), karşılaştıran çalışmalar sınırlıdır. Bu tez, diyetle oluşturulan DEA'nın geç gebelik sıçan miyometriyumunda **(i)** pasif bazal tonusu düşürüp düşürmediğini ve **(ii)** ritmik fazda toplam (AUC) azaltıp azaltmadığını test etmektedir. Hipotez, DEA grubunda bazal gerilimin daha düşük ve ritmik faz AUC'nin daha düşük olacağı yönündedir. Sprague–Dawley damlarda (geç gestasyon) kontrol ve DEA diyetleri uygulandı. Uzunlamasına miyometriyum şeritleri organ banyosunda izometrik olarak kaydedildi ; denge döneminden sonra bazal tonus ve AUC analiz edildi. Beş ardışık fazdan (Başlangıç, Bazal, Ritmik, Final) bazal ve ritmik kesitler analiz edildi. Birincil sonlanım 600 saniyelik ritmik faz |AUC|; ikincil ölçümler ortalama gerilim, tepe kuvvet ve frekanstı. Dağılıma göre parametrik veya nonparametrik testler kullanıldı. Teknik gürültüyü azaltmak için her dâmdan en iyi tek kanal seçildi; odaklı karşılaştırmada kontrol n=6, DEA n=6 kullanıldı. Tüm kanallar dahil edildiğinde sıfıra yakın AUC değerlerinin fazlalığı nedeniyle grup farkı istatistiksel olarak belirginleşmedi. Kontrol grubunda bazal→ritmik geçişte ortalama gerilim ve |AUC| anlamlı arttı; DEA'da yalnızca az sayıda şeritte düşük genlikli aktivite gözlendi. Frekans ölçütü, DEA'daki çok küçük genlikli "titreme"lerin sayımı nedeniyle ayırt edici olmadı. Bu çalışma, maternal DEA'nın miyometriyal pasif tonu ve spontan kasılma işini derin biçimde azalttığını nicel olarak göstermektedir. Bulgular, DEA'nın doğum eyleminde yetersiz uterus gücüne ve olası ilerlememe sorunlarına katkıda bulunabileceğini desteklemektedir. Klinik açıdan gebelikte DEA'nın erken taranması ve düzeltilmesi, yalnızca hematolojik değil, uterin biyomekanik açıdan da kritik olabilir.

Anahtar Kelimeler: Alan altı (AUC), demir eksikliği anemisi, gebelik, miyometriyum, organ banyo deneyleri, uterin kontraktilite.

ABSTRACT

Iron and Uterine Contraction: An Experimental Investigation of the Effect of Iron Deficiency Anemia on Myometrial Contraction

Iron-deficiency anemia (IDA) is highly prevalent in pregnancy and linked to adverse outcomes, yet its direct impact on late-gestation myometrial passive tone and spontaneous contractility has not been quantified rigorously. Prior work emphasizes stimulated or amplitude-based responses, with limited, artifact-controlled comparisons of passive uterine tone and rhythmic-phase contractile work (AUC) under IDA versus iron-replete conditions. This thesis tests whether diet-induced IDA (i) lowers baseline passive tension and (ii) markedly reduces spontaneous contractile work during the rhythmic phase in late-pregnant rat myometrium. The priori hypothesis predicted lower resting tone and smaller rhythmic-phase AUC in IDA than in controls. Pregnant Sprague–Dawley dams received control or IDA diets. Longitudinal myometrial strips were recorded isometrically in organ baths across five sequential phases; analyses focused on Baseline and Rhythmic segments. The primary endpoint was the absolute 600-s rhythmic-phase |AUC|; secondary metrics were mean tension, peak force, and frequency. Assumption-appropriate tests were used (paired t/Wilcoxon within strips; Mann–Whitney or Welch t between groups). To minimize technical noise and within-animal duplication, one best strip per dam (highest rhythmic |AUC|) was selected; the focused comparison used n=6 controls vs n=6 IDA. When all channels were pooled, numerous near-zero AUC records (especially in IDA) obscured group differences. Controls showed significant baseline-rhythmic increases in mean tension and |AUC|, consistent with robust spontaneous activity. IDA strips were largely quiescent; in a minority, very high counts of tiny twitches inflated frequency but contributed negligible work, making frequency a poor discriminator. The study demonstrates that maternal IDA profoundly depresses myometrial passive tone and spontaneous contractile work in late pregnancy. This biomechanical deficit offers a mechanistic basis for labor dysfunction associated with IDA and underscores the clinical importance of early detection and correction of iron deficiency to support effective uterine performance at term.

Keywords: Area under the curve (AUC), iron-deficiency anemia, myometrium, organ bath, pregnancy, uterine contractility

1. INTRODUCTION and AIM

Iron deficiency anemia (IDA) is the most common form of anemia and a significant global health issue, affecting over a third of the world's population and posing major public health challenges, especially in developing countries (1, 2). Global and regional studies indicate that IDA is a common nutritional issue, particularly among vulnerable groups such as infants and pregnant women (3, 4).

With nutritional deficits accounting for half of the cases worldwide, IDA disproportionately affects women of reproductive age, pregnant and lactating women, and young children, leading to severe health consequences if untreated (5). In rural areas of the Mediterranean region, awareness of iron deficiency as a cause of anemia was relatively high, with 71% of survey participants recognizing the link; yet there remains a need for increased education on iron-rich diets (6).

While the prevalence of anemia among women aged 15–49 decreased from 2000 to 2013, this trend reversed, increasing from 2013 to 2019, though severe anemia declined globally during this period (7). Despite a general decrease in anemia prevalence from 1990 to 2019, population growth has led to an increase in the total number of cases (8). This rise in prevalence after 2013 highlights challenges in sustaining progress against IDA, suggesting that current interventions may be inadequate or poorly implemented, emphasizing the need for stronger interventions to meet Global Nutrition Target 2, which aims for a 50% reduction in anemia among women of reproductive age by 2025 (9). Failure to meet this target could exacerbate health disparities and economic burdens in affected countries. A coordinated global effort is necessary, involving healthcare practitioners, dietitians, and policymakers to implement evidence-based interventions and promote self-care practices for prevention and management (10, 11)

The causes and risk factors of IDA during pregnancy are multifaceted, including increased physiological iron demands, inadequate dietary intake, and conditions impairing iron absorption (12, 13). During pregnancy, the demand for iron surges due to the expansion of the maternal red blood cell mass and the needs of the developing fetus and placenta, requiring approximately 1,000 mg more iron (13). Many women enter pregnancy with depleted iron stores, exacerbated by factors such as short interpregnancy intervals, heavy menstrual bleeding, and previous pregnancies (14).

IDA during pregnancy has serious physiological implications for both maternal and fetal health, including increased risks of preterm labor, low birth weight, maternal morbidity, fatigue, weakness, pallor, and increased susceptibility to infections due to impaired immune (15-17). Iron deficiency can also impair fetal neurodevelopment, increasing the risk of developmental delays and cognitive deficits (18). Moreover, IDA significantly affects uterine contractions due to iron's role in muscle function and oxygen transport, increasing the risk of adverse pregnancy outcomes and labor complications (19-21).

Epidemiological studies in Türkiye (22-24) have highlighted a high prevalence of IDA among various demographic groups, with rates varying significantly. In Southeastern Anatolia, a study on reproductive-aged women found a 36% prevalence of anemia, with iron deficiency being a major contributing factor, particularly among seasonal agricultural workers and those with lower educational levels (25). In Kahramanmaraş, 23.8% of women aged 19–40 years were affected (22). Similarly, in Kocaeli, 9.7% of adolescent girls were anemic, with 88.2% of these cases due to iron deficiency (24). Factors such as maternal education and socioeconomic status significantly influence adherence to iron supplementation, which in turn affects the prevalence of IDA (26).

On the cellular level, the differential expression and activity of ion channels are critical to the transition from uterine quiescence to the contractile state required during labor (27). The resting membrane potential (RMP) of myometrial smooth muscle cells (MSMCs) is critical for this transition. This transition is influenced by ion channels, such as ATP-sensitive potassium channels (KATP) and Na^+-activated K^+ channels (SLO2.1), which modulate membrane potential and excitability (28, 29). KATP channels, for instance, are significant in regulating myometrial excitability by modulating ion conductivity, affecting the frequency and amplitude of uterine contractions (28). Altered ion channel function or dysregulated RMP can pose significant risks to maternal and fetal health (30).

In smooth muscle cells, IDA can potentially alter the ionic balance and energy metabolism within uterine myocytes (31). Iron influences ATP production and calcium channel regulation, both critical for muscle contractility (32). Alterations in ATP availability and calcium-dependent signaling pathways can lead to complications in excitability and contractility (33). Furthermore, iron deficiency can exacerbate skeletal muscle dysfunction, contributing to symptoms such as dyspnea and reduced exercise capacity in heart failure

patients, primarily due to intracellular iron depletion (34). Similarly, IDA also affects smooth muscle function, which is vital for supporting uterine tone and facilitating labor (35).

IDA can affect uterine blood flow, as the uterus relies on adequate arterial supply to support pregnancy (36). Arterial blood supply is primarily provided by the uterine arteries, supplemented by the ovarian and vaginal arteries, with ipsilateral and contralateral anastomoses present (37). This vascular dynamic shifts between the follicular and luteal phases, adjusting blood flow as needed for reproductive processes (38).

During pregnancy, the uterus undergoes significant changes, including increased blood flow, hormonal adjustments, and structural remodeling to support the developing fetus (39). The increase in uterine blood flow during pregnancy is dramatic, with a 30-50 fold increase compared to the nonpregnant state, primarily due to decreased vasomotor tone and increased endothelial vasodilator production (40).These changes are facilitated by the remodeling of uterine arteries and the interaction between endothelial and vascular smooth muscle cells, with perivascular adipose tissue playing a crucial role in regulating vascular reactivity (41). This enhanced blood flow is crucial for fetal growth and adequate oxygenation, as demonstrated in studies where increased uterine artery blood flow correlated with improved fetal oxygen delivery and growth (42). Therefore, the efficient transport of oxygen becomes a pivotal aspect of uterine function during pregnancy.

Consequently, oxygen transport becomes essential for maintaining uterine function, as it influences overall cellular metabolism, which is vital for reproductive health (43, 44). Disruptions in oxygen delivery can lead to hypoxia. Hypoxia, or reduced oxygen availability, plays an important role in modulating uterine contractility and excitability. During labor, intermittent hypoxia occurs due to myometrial contractions compressing blood vessels, which can limit ongoing contractions and prevent fetal distress by decreasing excitability and intracellular calcium concentration (45). Hypoxic pregnancy led to increased uterine artery constrictor reactivity (46).

However, IDA may disrupt these adaptive oxygenation mechanisms, as iron is essential for oxygen transport via hemoglobin. According to Peebles (47), these adaptations guarantee adequate nutrient and oxygen delivery to the fetus while providing a protective environment. The interplay between blood flow and vascular resistance, therefore, becomes crucial for optimal fetal development. He emphasizes the importance of fetal cardiovascular

and metabolic responses to hypoxemia for fetal survival, particularly during events like human labor, where transient fetal hypoxemia occurs due to uterine contractions (47).

Building upon the significance of oxygen transport and its impact on uterine function, emerging research using advanced electrophysiological techniques has provided valuable insights into the ionic currents contributing to the resting membrane RMP and how they are modulated during pregnancy in both humans and animal models like Sprague-Dawley rats (48). These uterine contractions are regulated by spontaneous action potentials that alter cell and tissue electrical excitability, although the exact mechanisms of pacemakers and synchronization remain incompletely understood (49). Electro myometrial imaging and vector analysis have been used to study the electrophysiological origins of labor contractions, revealing that phasic contractility is a product of slow and fast wave biopotentials, which are crucial for myometrial contractile responses. These studies suggest that slow waves have a downward directionality towards the cervical opening, which may help predict delivery timing and gestational pathologies (50, 51). The uterus achieves the synchronized contractions necessary for labor via increased myocyte connectivity through gap junctions and heightened excitability, enabling effective fetal expulsion. Parturition highlights the ability of the uterus to undergo dramatic physiological changes, including synchronization of myocyte contractions leading to the necessary intrauterine pressure for labor and the eventual expulsion of the fetus (52).

Despite these advancements, many aspects of parturition remain poorly understood, particularly the precise mechanisms that trigger the onset of labor (53, 54). The mechanisms of initiation and regulation of labor activity are still insufficiently studied, indicating a need for further research to fully understand these processes and their implications for labor outcomes (55, 56). Understanding these mechanisms can inform clinical practices aimed at improving outcomes in high-risk pregnancies, particularly in managing conditions that may compromise fetal oxygenation (57, 58). Ongoing research is essential to unravel the complexities of uterine physiology, which will lead to improved maternal and fetal health outcomes (59). Many existing theories on labor initiation and regulation are considered to be of historical interest, suggesting that there is a gap in contemporary understanding and the need for updated research that reflects current scientific knowledge and advancements (55).

Given the critical role of iron in muscle function and the modulation of uterine excitability, there is a pressing need to understand how IDA affects the electrophysiological properties of uterine myocytes. Research continues to uncover the molecular and cellular mechanisms that govern uterine physiology and its associated pathologies, advancing our therapeutic approaches for gynecological conditions (60). Understanding the uterus's physiology—including its vascular regulation and contractile behavior—is key to addressing various reproductive health challenges such as infertility, menstrual disorders, and complications during pregnancy (61).

Similarly, diet-induced obesity has been reported to impair spontaneous myometrial contractility, leading to reduced peak force and diminished area under the curve (AUC). Although anemia contributes to maternal morbidity through hypoxia at the cellular level, its association with postpartum hemorrhage remains debated. Omotayo et al. reviewed 13 studies examining this relationship (62). They found that severe prenatal anemia significantly increased postpartum hemorrhage risk (OR = 3.54; 95% CI: 1.20–10.4; p = 0.020), while mild (OR = 0.60; 95% CI: 0.31–1.17; p = 0.130) and moderate anemia (OR = 2.09; 95% CI: 0.40–11.1; p = 0.390) did not yield statistically significant associations (62).

In another research, Muir et al. (2016) used a model of diet-induced obesity by feeding female rats a high-fat, high-carbohydrate diet for six weeks prior to conception and during pregnancy (term = 22 days; n = 20/group). Uterine contractility was assessed ex vivo for 30 minutes, with analysis of contraction frequency (cycles/min), peak amplitude, and integrated tension (63).

To investigate the mechanistic basis and clinical outcomes of uterine contractions observed in term pregnant women undergoing intravenous iron therapy, Halilzade et al., 2024 conducted a study involving 136 women beyond 35 weeks of gestation diagnosed with IDA, where participants received IV iron treatment and underwent nonstress testing both pre- and post-intervention. Their findings indicate that transient regular uterine contractions post-IV iron may predispose to early-term labor in cesarean patients. Confirmation via prospective human and preclinical models is warranted. It is worth noting that, of the original 159 patients in Halilzade et al., 2024, 23 were excluded due to baseline nonstress test contractions (33).

Most existing research has concentrated on factors influencing active myometrial contractions, with comparatively little focus on how IDA shapes passive uterine tone. This work hypothesizes that dietary iron restriction in dams accelerates the transition from quiescence to a labor-like contractile state, potentially amplifying pre-labor excitability. Such changes, absent in IDA controls, may provide a mechanistic explanation for increased preterm birth risk and greater clinical intervention rates. By targeting the resting membrane potential of individual myocytes in the Sprague-Dawley model, the study examines how iron deficiency perturbs smooth muscle electrophysiology and, by extension, parturition mechanisms (64, 65).

The main objective of this research was to determine how an IDA (iron deficiency anemia) diet alters the contractile function of the rat uterus, particularly in late pregnancy. In other words, this thesis aims to find out if iron deficiency directly affects myometrial (uterine smooth muscle) contractility.

The central hypothesis posits that dams fed an IDA diet will exhibit lower baseline passive tension (resting uterine muscle tone) and a tendency toward earlier or more pronounced spontaneous contractions compared to dams on a normal iron-sufficient diet. This means an IDA myometrium may transition from a quiescent (resting) state to active, labor-like contractions sooner or more intensely than normal, potentially predisposing to premature labor.

This hypothesis is grounded in observations that iron deficiency can impair muscle function in general and in clinical correlations where maternal IDA is linked to a higher risk of preterm birth. However, until now, the direct impact of iron levels on uterine muscle behavior has not been well studied. By analyzing the baseline tension and spontaneous contraction patterns of uterine strips from IDA versus control rats, it was expected to observe the predicted differences – for example, that baseline passive tension in IDA-fed dams would be lower than that of dams on a normal diet, consistent with our hypothesis.

This thesis's experimental design was developed beginning with a review of pertinent literature, leading to the establishment of a research hypothesis and contextual framework. The empirical section integrates biological material handling — initiated through ethical animal use — followed by anatomical dissection and organ bath analysis to capture contractile dynamics of myometrial strips. Key quantitative contractility parameters were

defined for subsequent analysis: (i) Baseline resting (passive) tension – the resting force (in milligrams) maintained after full equilibration, in the absence of contractions; (ii) Peak contractile force – the maximum force generated during any contraction; and (iii) Contraction frequency and amplitude – when repeated spontaneous contractions occurred, the frequency (contractions per minute) and typical strength (peak-to-peak amplitude) were measured. Data analysis spanned from exploratory to metric-specific domains, forming the basis for results interpretation. These findings are contextualized within the broader literature, with an emphasis on limitations and avenues for continued inquiry.

.

2. GENERAL INFORMATION

2.1. Anatomy and Histology of the Uterus

The human uterus is a hollow, pear-shaped organ located in the female pelvis, as shown in Figure 1. It is crucial for gestation, menstruation, and labor (66). The size and shape of the uterus vary with age and fertility, influenced by both physiological and pathological factors. Uterine size increases during childhood and adolescence, reflecting the influence of puberty, and continues to grow slowly during adult life until around the age of 40, after which it begins to decrease, particularly around menopause (67, 68).

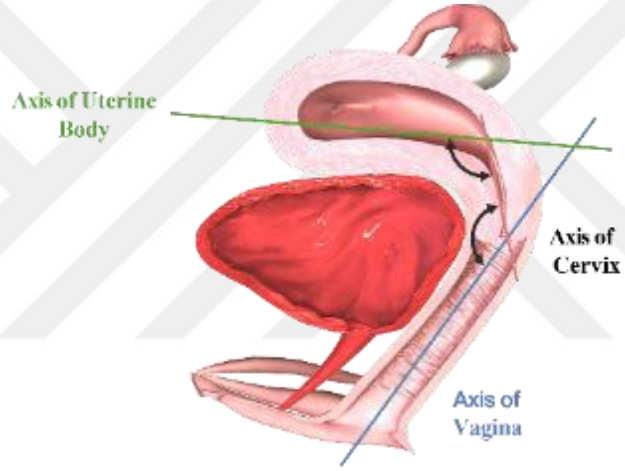

Figure 1. The anatomical relationships of the uterine body, cervix, and vagina axes, detailing the angles of anteflexion and anteversion important for understanding uterine positioning in relation to the pelvic structure (69).

As shown in Figure 2, the uterus is divided into four main segments: fundus, corpus (body), isthmus, and cervix (66, 70). The fundus, at the top of the uterus, is a broad, curved area where the fallopian tubes enter, crucial for ovum entry. The corpus, extending from below the fallopian tubes to the isthmus, constitutes the main body of the uterus and is the primary site for implantation and gestation. The isthmus serves as a narrow neck linking the corpus to the cervix, facilitating communication between the uterine cavity and the cervical canal. The cervix, opening into the vagina, includes the internal and external os, regulating passage between the uterus and the external reproductive tract (70).

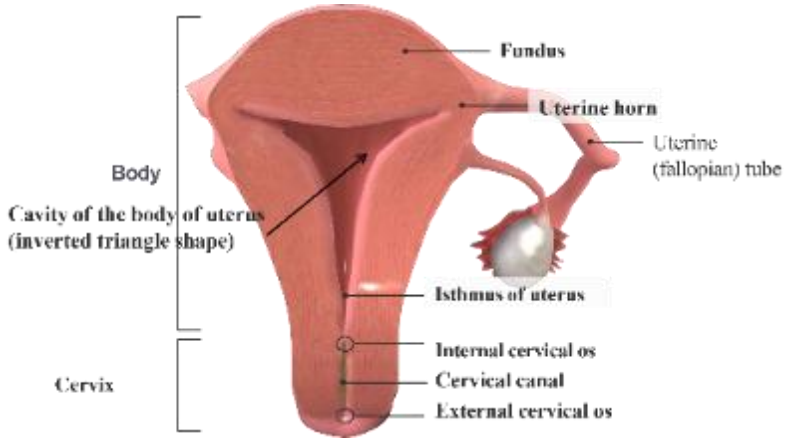

Figure 2. Anatomical structure of the uterus showing divisions into fundus, corpus, isthmus, and cervix (69).

Figure 3 illustrates a cross-section of the uterine layers. The structural composition of the uterine wall consists of three layers, as shown in Figure 3: the endometrium (inner lining), the myometrium (thick muscular middle layer), and the perimetrium (outermost protective layer) (71).The endometrium, the inner mucosal layer, is vital for implantation and pregnancy support. The myometrium, consisting of smooth muscle, facilitates uterine contractions and wall strength. The perimetrium, the outer protective layer, ensures structural integrity (71). Understanding this anatomy is crucial for examining IDA effects on uterine myocytes, as changes in the myometrium may impact contractions and pregnancy adaptations (72).

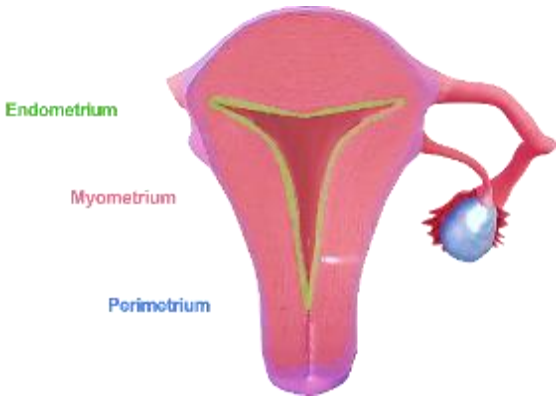

Figure 3. Anatomical illustration of the uterus showing the endometrium, myometrium, and perimetrium layers, which play essential roles in uterine function, pregnancy, and response to physiological stimuli (69).

The myometrium, the muscular layer of the uterus, plays a crucial role in stabilizing the uterus during pregnancy owing to its unique anatomical and histological features. It is primarily responsible for the contractile function of the uterus, essential for implantation, fetal growth, and parturition (73). Histologically, the myometrium is composed of smooth muscle fibers arranged in three layers in different directions, which allows for complex contractile movements necessary during labor and delivery (74). These layers enable the uterus to contract effectively during childbirth.

Furthermore, the zonal anatomy of the myometrium, characterized by a distinct junctional zone that differs structurally and functionally from the outer myometrium, serves a supportive function during early pregnancy and becomes increasingly important as the uterus adapts to accommodate the developing fetus and during parturition (73). During pregnancy, the myometrium is maintained in a quiescent state due to inefficient cell-to-cell coupling and the inhibitory influence of nitric oxide, which minimizes contractile activity as gestation progresses (75). This quiescence is essential for maintaining the structural integrity of the uterus and preventing premature contractions.

The role of the myometrium extends beyond pregnancy, as it helps prevent excessive loss postnatally (73). The myometrium's interaction with the uterine vasculature and its anatomical relationships, such as with the ureter, are also important considerations, especially in surgical contexts, such as hysterectomy, where the risk of injury is present (70). Figure 4 provides a detailed schematic of the uterine wall layers, highlighting the vascular and structural features of the myometrium.

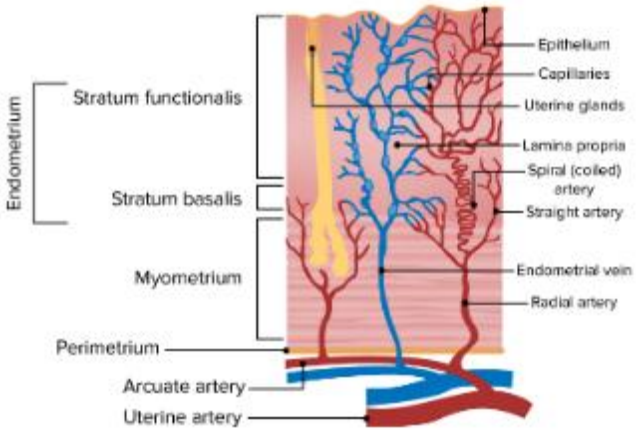

Figure 4. Detailed anatomical depiction of uterine layers, highlighting endometrial glands,spiral and straight arteries, and the myometrial and perimetrial tissues. This image illustrates key structures involved in uterine vascularization and tissue dynamics (69).

Figure 4 depicts the anatomical and vascular structure of the uterine wall, including the endometrium, myometrium, and perimetrium. Overall, the myometrium is a dynamic and essential component of the uterus, and its anatomy and histology are intricately linked to its function and the broader reproductive health of women.

2.2. Physiology of the Uterus

A systematic analysis of pregnancy physiology highlights how physiological changes impact clinical practice and their connection to pregnancy-related disorders .The primary function of the uterus is to accommodate and nurture a fertilized ovum until it reaches full gestation .During pregnancy, the uterus undergoes significant changes, including increased blood flow, hormonal adjustments, and structural remodeling to support the developing fetus (39).

Peebles (2012) argues that these adaptations guarantee adequate nutrient and oxygen delivery to the fetus while providing a protective environment. The interplay between blood flow and vascular resistance is crucial for optimal fetal development. Peebles emphasize the importance of fetal cardiovascular and metabolic responses to hypoxemia for fetal survival, particularly during events like human labor, where transient fetal hypoxemia occurs due to uterine contractions (47).

Understanding these mechanisms can inform clinical practices aimed at improving outcomes in high-risk pregnancies, particularly in managing conditions that may compromise fetal oxygenation (57). The uterus's vascular supply, primarily from the uterine artery with contributions from the ovarian artery, supports hormonal regulation and uterine function. This vascular dynamic shifts between the follicular and luteal phases, adjusting blood flow as needed for reproductive processes (1).

Research continues to uncover the molecular and cellular mechanisms that govern uterine physiology and its associated pathologies, advancing our therapeutic approaches for gynecological conditions (60). In summary, understanding the uterus's physiology—including its vascular regulation and contractile behavior—is key to addressing various reproductive health challenges such as infertility, menstrual disorders, and complications during pregnancy (61).

2.3. Uterine Myocytes

Uterine myocytes, the primary smooth muscle cells in the myometrium, are crucial for uterine function, particularly in contraction and relaxation during labor and pregnancy maintenance, exhibiting intrinsic pacemaker activity and rhythmicity influenced by various factors (77). During parturition, increased myocyte connectivity via gap junctions enhances excitability and synchronizes contractions to generate intrauterine pressure for fetal expulsion (52). Contractions are regulated by spontaneous action potentials (AP) that alter cell and tissue electrical excitability through pacemaker and synchronization mechanisms (30).

Electrical activity, particularly APs and calcium signaling, underpins contractile function and facilitates uterine transitions from quiescence to an active state, with dysfunction in ion channels or RMP resulting in significant maternal and fetal health risks (30).

Differential ion channel expression and activity are essential for transitioning from uterine quiescence to the contractile state required during labor (27). Electro-myometrial imaging and vector analysis have demonstrated that labor contractions' electrophysiological origins involve slow and fast wave biopotentials crucial for myometrial contractile

responses, contributing to the prediction of delivery timing and gestational pathologies (50, 78).

The unique structural features of uterine myocytes, including the arrangement of contractile proteins, ion channels, and gap junction connectivity, enable coordinated and forceful contractions (79). Uterine myocytes maintain quiescence during most pregnancy through mechanisms that prevent premature contractions, such as progesterone influence and ion channel activity regulation (80).

2.4. IDA and Its Impact on Cellular Physiology

Iron is essential for hemoglobin-mediated oxygen transport and for iron-containing enzymes in cellular respiration. During pregnancy, IDA affects up to 50 % of women and produces fatigue, reduced exercise tolerance, and systemic hypoxia (81). In the rat model, prolonged low-iron feeding (≤ 3 ppm Fe) reliably induces IDA, characterized by lower hemoglobin, hematocrit, and tissue iron stores (82).

In the gravid uterus, the myometrium maintains a basal resting tone and generates coordinated contractions at parturition under hormonal control. Resting tension reflects intrinsic myocyte tonicity and primes the tissue for activation, while active contractions (elicited ex vivo by agents like oxytocin) display quantifiable changes in frequency, amplitude, and area under the AUC (83).

IDA-induced hypoxia compromises myocyte bioenergetics and calcium handling, leading to altered contractile dynamics. In IDA Sprague-Dawley rats, resting tension is reduced by up to 25 %, peak contraction frequency decreases, and AUC is significantly attenuated compared to controls (84).

Chung et al. demonstrated in mice that IDA downregulates ryanodine receptor 2 and inhibits the sarcoplasmic/endoplasmic reticulum Ca^{2+}-ATPase (SERCA) pump, causing reduced contractile function (88). Frass et al. found that women with moderate-to-severe IDA (Hb < 10 g/dL) had a significantly higher incidence of uterine atony and subsequent postpartum hemorrhage after cesarean delivery (90). Such contractile deficits may predispose to uterine atony and preterm labor in IDA pregnancies.

2.5. Original Value of Research

Existing studies focus on active uterine contractions, while passive tone changes under IDA remain underexplored. This study proposes that iron restriction in dams promotes early transition to a labor-like state, raising pre-labor excitability—changes not seen in iron-sufficient controls. These findings may explain higher preterm birth risks and interventions. The study investigates resting membrane potential alterations in Sprague-Dawley uterine myocytes to uncover electrophysiological disruptions caused by IDA (64, 65).

The central aim of this study is to assess whether dietary iron deficiency directly alters the contractile behavior of the myometrium during late-stage pregnancy. Pregnant Sprague-Dawley rats are used for their reproducible hematological and serum profiles, providing a consistent model for evaluating how IDA influences smooth muscle physiology (87). Prior work, such as Gáspár et al., 2022, applied this model to investigate obesity-related shifts in uterine contractility using a high-fat, high-sucrose diet (88). Given the clinical relevance of preterm labor and related complications, this study addresses the need to understand how IDA affects uterine myocyte excitability and contractile properties, aiming to establish a direct link between iron deficiency and impaired myometrial function.

Studying IDA's effect on myometrial contractility in pregnant Sprague-Dawley rats helps uncover how iron deficiency influences uterine excitability and risk of preterm labor. To determine whether iron deficiency exerts a direct effect on myometrial contractility, this thesis utilizes the Sprague-Dawley rat model, which offers advantages such as short estrous cycles and high responsiveness to genetic and pharmacological interventions. Despite these strengths, extrapolation to human obstetrics necessitates systematic benchmarking across critical parameters: passive tension, contraction frequency, and the AUC.

In this study, rat uterine horns from virgin non-pregnant animals were mounted at approximately 0.5 g to sustain spontaneous contractile activity. In contrast, horns from proven breeders required only 0.3–0.4 g, reflecting increased Ca^{2+} sensitivity associated with parity (89). For human myometrium, term-pregnant lower segment strips are generally preloaded at 2–3 g to approximate *ex vivo* conditions, whereas non-pregnant tissue equilibrates at 1–1.5 g, due to structural differences such as connective tissue composition and uterine geometry (90).

3. MATERIALS and METHODS

This thesis quantifies the baseline resting tension of the myometrium in timed-pregnant Sprague Dawley dams subjected to IDA compared with those maintained on a standard diet. In addition, key contractile parameters spontaneous contraction frequency and area under the curve (AUC) are analyzed. Although myometrial contractility has been extensively studied, a rigorous, quantitative assessment of resting tension under iron-deficiency anemia during pregnancy remains lacking and, as noted, the direct effect of iron deficiency on uterine contractility has not previously been focused upon.

Table 1 presents the methodological structure underpinning the experimental design. Timed-pregnant Sprague–Dawley rats in late gestation (uterine tissue collected at GD21) were used; GD20 in this strain closely resembles human late-third-trimester physiology while preceding labor-induced remodeling (88).

Two diet groups were defined: IDA (low-iron purified chow containing approximately 3–4 mg Fe·kg^{-1} feed) and control (matched formulation containing 168 mg Fe·kg^{-1} feed). This low-iron paradigm has been reported to induce maternal anemia with low mortality in pregnant rats (91, 92). Sample size was set at 8 dams per group, providing 80 % power to detect a 25 % change in passive tension (SD = 12 %, $\alpha = 0.05$), informed by prior uterine preload variance data (49). In the present study, biochemical verification of anemia on GD20 was based on maternal hematocrit; hemoglobin, ferritin, and transferrin saturation were not available. Dams whose Hct did not fall below the pre-specified anemia threshold were excluded from the IDA cohort, and the threshold was chosen on the basis of published criteria for clinically meaningful anemia in pregnancy (33).

Table 1. Experimental methodology

Factor	**Details**	**Rationale**
Species (day of gestation)	Sprague-Dawley rats, GD 21	GD21 in this strain approximates human late third-trimester physiology while still preceding term labor, avoiding confounding labor-induced myometrial remodeling.
Diet groups	IDA: purified chow (e.g. TD.80396) containing ~4 mg Fe·kg^{-1}, started before mating and maintained throughout gestation. **Control:** matched formulation (e.g. TD.80394) containing 168 mg Fe·kg^{-1}.	Nutrient-matched low-iron chow at ~4 mg Fe·kg^{-1} reliably reduces maternal hematocrit into the anemic range with low mortality, while 168 mg Fe·kg^{-1} maintains iron sufficiency in pregnant dams.
Sample size	8 dams per group (power = 0.8 to detect a 25 % change in passive tension, SD ≈ 12 %, α = 0.05).	Power calculation based on variance reported for rat uterine preload studies (passive-tension SD ≈ 12 %), ensuring sensitivity to detect physiologically relevant shifts in baseline tone.
IDA verification	Maternal hematocrit (Hct) measured on GD20; dams with Hct below a pre-specified threshold were classified as IDA, and those above the threshold were excluded from the IDA cohort.	Hematocrit-based classification provides hematological confirmation of anemia and prevents misclassification, within budget constraints that precluded full iron-panel testing. The Hct cut-off was chosen to approximate clinically significant IDA (≈ Hb < 10 g·dL^{-1}).

This experimental model isolates strip uterine muscle biomechanics under IDA diet (Figure 5) rat fed versus control conditions using an in vitro organ-bath assay, paired with cellular-level electrophysiological validation. The primary endpoint is passive (resting) tension, operationalized as the mean force during a stable, contraction-free 60-second period post-preload equilibration. Secondary parameters include maximum force generation, contraction rate, latency to initial contraction, and total contractile output (measured by AUC). The in vitro configuration circumvents endocrine, vascular, and immune modulators, thereby isolating dietary impacts on uterine muscle compliance and excitability.

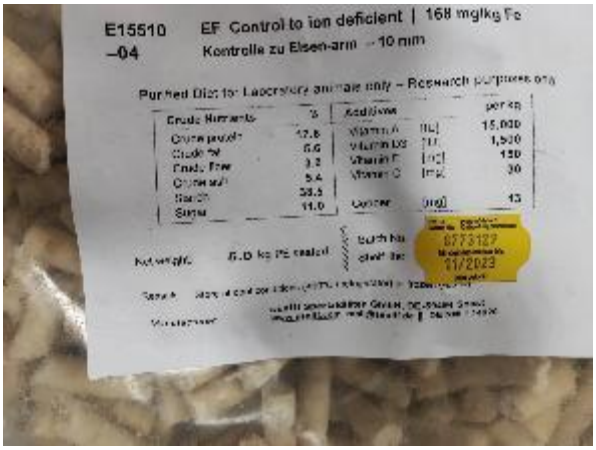

Figure 5. Close-up of the label on the iron-deficient purified diet bag, showing product code E15510 ad iron content 168 mg/kg Fe, with a nutrient/additive table.

3.1. Experimental Design

The project followed an integrated workflow that began with ethically approved animal procurement and culminated in isolated organ recordings of uterine strips (Figure 6). After confirming animal welfare and allocating rats to dietary regimens, myometrial tissue was excised, mounted in a four-channel organ-bath system, and equilibrated under 03-04 g passive tension for 60 minutes. Continuous force was acquired with BIOPAC Student Lab at 1 kHz, providing baseline tone and spontaneous-contraction profiles. In light of the objective to examine IDA-induced modulation of spontaneous myometrial function during advanced gestation, the dataset was constrained to dam uteri exclusively. Therefore, the final comparison focused on control-diet pregnant versus IDA strips. Occasional force-transducer failures reduced the number of active baths per recording to two or three; missing channels were documented but not replaced. Data analysis was conducted using BSL Analysis software (Biopac Student Lab Analysis v1.4.7), which allowed inspection of each .acq file and extraction of key metrics: baseline passive tension, peak contractile force, and contraction frequency.

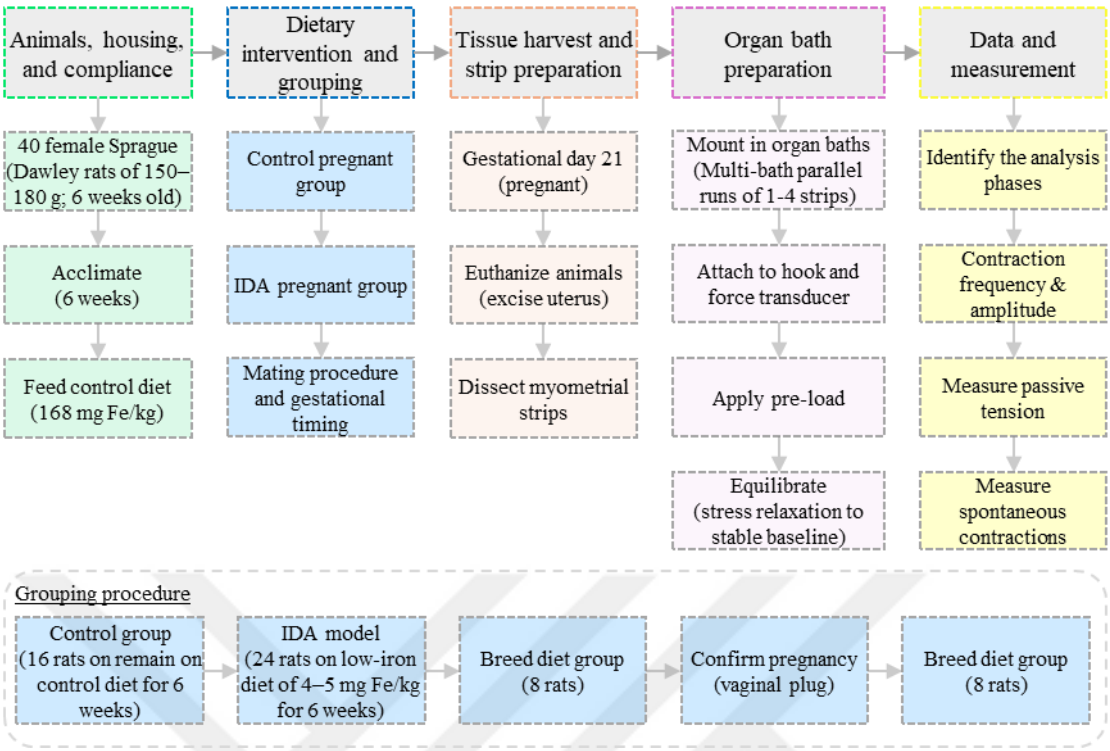

Figure 6. Experimental workflow

3.2. Animals, Housing, and Ethical Compliance

Young adult female Sprague–Dawley rats (PND 36; 150–180 g) were procured from the Karadeniz Technical University (KTÜ) Surgical Research Centre and housed in groups of 3–4 under standardized environmental conditions (22 ± 2 °C; 55 ± 10% RH; 12-hour light/dark cycle) with unrestricted access to food and water. All experimental protocols were approved by the KTÜ Local Animal Experiments Ethics Committee under the study titled Iron and Uterine Contractility: An Experimental Investigation of Effects of IDA on Myometrial Contractility. Only data from dams in the control group and IDA groups were included in the current analysis. Files with fewer than four active organ baths were accepted if signal integrity conformed to predefined standards—namely, a stable baseline, identifiable contractile events, and absence of recording artifacts.

While previous investigations have employed varied sample sizes, Akgün-Ünal et al. (2021) evaluated the effects of dietary zinc on rat myometrial contractility using 20 animals allocated to four distinct groups (93). The Budgetary constraints limited the present study to 40 rats; ultimately, 36 pregnant animals produced usable strips (control group on normal diet

= 30, IDA = 6). Originally proposed iron-supplemented groups (ID+Fe-F and ID+Fe-P, 80 mg kg^{-1} Fe, s.c.) were excluded from this phase and will be included in future experiments. Furthermore, experimental recordings were carried out using four parallel organ baths. Owing to transducer malfunctions, two to four active channels were available per session. All valid recordings were retained, and missing channels were appropriately annotated.

3.3. Dietary Intervention and Grouping

Two nutritionally equivalent pelleted diets were utilized: TD.80394 (control; 168 mg Fe kg^{-1}, 0.6 % phosphate; Lot E15510-04) and TD.80396 (IDA; ~4 mg Fe kg^{-1}; Lot E15510-24), both isocaloric and prepared by ssniff Spezialdiäten GmbH. All animals underwent a standardized 6-week run-in on TD.80394 before randomization to either continue on the control diet or transition to the IDA formulation for an additional 6 weeks. Thus, the 12-week feeding protocol was designed to induce pre-gestational iron depletion while maintaining equivalent nutrient composition. Supplier documentation and nutritional analysis confirmed macronutrient and phosphate parity. For final analysis, only pregnant rats were included, with the IDA cohort further divided into organ-bath contractility and single-cell electrophysiology subgroups (n = 8).

3.4. Mating Procedure and Gestational Timing

Female rats in estrus or proestrus were paired with fertile males on a control diet overnight. Gestational day 0 was confirmed by presence of a vaginal plug or sperm. All pregnancies progressed on the assigned diet until term (22 days).

Where relevant, trivalent iron (Monofer®/Ferinject®) was injected subcutaneously at 80 mg/kg on mating day, and again at gestational day 14. Mating at 6 weeks was selected to coincide with the iron-depletion timeline. In contrast, other studies mated 9-week-old females (88) or used a 6-week pre-mating diet to model obesity (63). The present protocol emphasized developmental consistency and timing of iron loss.

3.5. Hematological assessment and rescue iron dosing

Maternal anemia was monitored by microhematocrit measurement from tail-vein blood on GD20. Because of budget limitations, we could not perform a full iron panel

(hemoglobin, ferritin, transferrin saturation) and therefore used hematocrit as the primary classification criterion for anemia. Dams with Hct below the pre-defined threshold were classified as IDA; those above the threshold were allocated to the control group.

To minimize severe morbidity, a small number of dams whose hematocrit fell to critically low levels received a single “rescue” dose of iron sucrose (Ferrosel®, 100 mg/5 mL, Haver). The injection was administered subcutaneously with brief manual restraint, without general anesthesia, in accordance with the institutional ethics protocol. These dams were excluded from the main organ-bath contractility analysis but are reported descriptively in the hematology dataset.

3.6. Tissue Harvest and Strip Preparation

On gestational day 21, dams assigned to organ-bath studies were euthanized using an approved non-anesthetic method to avoid pharmacologic carryover effects on smooth-muscle function. The uterus was rapidly excised and transferred to ice-cold, carbogenated Krebs–Henseleit (KH) solution. To minimize any residual anesthetic effects on smooth-muscle tone, tissues underwent sequential washes followed by an equilibration period in the organ bath before recordings. A midline laparotomy was performed, and uterine horns were excised and placed in ice-cold, carbogen-aerated Krebs–Henseleit (KH) solution (composition in mM: NaCl 118.2; KCl 4.7; $MgSO_4 \cdot 7H_2O$ 1.2; $CaCl_2$ 1.6; KH_2PO_4 1.2; $NaHCO_3$ 25; glucose 5.5; EDTA 0.003). From the mid-horn—selected to avoid cervical specialization and fundal heterogeneity (88)—longitudinal myometrial strips (~7 × 1.5 × 1.0 mm) were dissected under stereomicroscopy. Decidua and serosa were carefully removed while preserving smooth muscle integrity. Strips were maintained in oxygenated cold KH until mounted. Each preparation was suspended vertically between a stationary support and a Grass FT-03 isometric force transducer in a 10 mL organ bath at 37 °C, pH 7.4, bubbled with 95 % O_2/5 % CO_2. All procedures and KH formulation were approved by institutional ethical review.

3.7. Organ Bath Preparation

Organ bath systems (Table 2) were used to assess uterine contractility. Each chamber had a capacity of 10 mL, jacketed and maintained at 37 °C. Aeration with a gas mixture of 95 % O_2 and 5 % CO_2 stabilized the bath at physiological pH 7.4. Force transducers were calibrated within a 0–5 g range, providing 1 mN resolution. Data were continuously sampled with PowerLab 26 T at 400 Hz and processed using LabChart version 8.

Table 2. Parameters for organ bath recordings.

Parameter	**Setting**
Bath volume	10 mL jacketed chamber at 37 °C
Aeration	95 % O_2 / 5 % CO_2 (pH 7.4)
Transducer calibration	0–5 g range, resolution 1 mN
Data capture	PowerLab 26 T @ 400 Hz; LabChart v8

Data were collected in real-time, cleaned, and subjected to both descriptive and inferential analysis. Parameters characterizing tissue responsiveness were extracted and compared. In the organ bath setup, myometrial strips were assessed under constant resting tension by securing one end to a fixed pin and the other to a force transducer. Contraction measurements proceeded in discrete phases (Figure 7): mounting the tissue, applying resting tension, capturing force through the transducer and converting it into digital signals, and allowing the tissue to equilibrate before stimulation.

Figure 7. Organ-bath measurement of myometrial contraction procedure

3.8. *Ex vivo* Mechanical Measurement of Myometrial Strips

To measure resting (passive) tension, myometrial strips are mounted isometrically between a fixed hook and a force transducer in a 10 ml organ bath containing Krebs-Henseleit solution (37 °C, pH 7.4) bubbled with 95% O_2/5% CO_2. Passive tension is set to 0.3-0.4 g and equilibrated for 60 min. Spontaneous contractions are recorded via a Biopac

MP150 system, sampling at 1 kHz; software computes peak frequency (contractions/min), amplitude, and area under the AUC, which together quantify basal tone, rhythmicity, and contractile workload (88)

Myometrial strips were suspended vertically in 10 mL jacketed glass baths (Çalışkan Cam, Türkiye), maintained at 37 °C, and continuously aerated with a 95% O_2 / 5% CO_2 gas mixture. One end was immobilized while the other was affixed to a BIOPAC FDT-05 isometric transducer connected to MP100 data acquisition. A 0.3-0.4 g preload was imposed, and the tissue was allowed to equilibrate for 60 minutes, with Krebs solution refreshed every 15 minutes, in strict adherence to protocol specifications.

To simulate *ex vivo* uterine stretches from fetal growth, a 1.0 g baseline passive tension was applied, and strips equilibrated for an additional 30 minutes. Stress relaxation typically caused a modest tension to decrease during this phase; the stabilized value defined the passive baseline tension (resting tone). No exogenous agents were introduced at this stage, allowing both resting tone and spontaneous contractile events to emerge under native physiological conditions.

3.9. Definition and Measurement of Resting (Passive) Tension

This study utilized the BIOPAC Student Lab system for signal acquisition and quantification. Force transducer signals were amplified and recorded using a BIOPAC data acquisition system (Biopac Student Lab, BSL). All analyses treated the animal as the statistical unit (strip-level values averaged per rat). The analog force signal, measured in milligrams or grams of tension, was continuously recorded. For each uterine strip, a tension-versus-time trace was obtained, displaying the baseline tone and any spontaneous contractions as a waveform. The statistical unit was defined as the individual animal, with values averaged across strips per subject.

Preload was defined as 0.5 g, representing the sarcomere length optimal for Sprague-Dawley myometrium (49). Equilibration was maintained for 60 min with readjustments at 15-min intervals. A stable 60-s, contraction-free segment post-equilibration was used for analysis. Passive tension was derived as mean isometric force (mN), normalized to tissue cross-sectional area (mN mm^{-2}) to correct for hypertrophy (88). Strips were retained only if they achieved ≥0.4 g active response to 60 mM KCl; <5 % failed. For passive compliance,

subsets (n = 6 dams/group) were subjected to graded stretch (0.1 g steps every 60 s to 1 g), and the slope of the tension–length curve (ΔT/ΔL) was compared across dietary groups (88).

Recordings were obtained from two to three strips simultaneously, creating multi-channel outputs. In total, 36 experiments were completed; IDs 6-1, 7-1, 16-2, 23-3, 31-4, and 32-4 were IDA, with the remainder control. Hardware malfunctions occasionally reduced recording capacity, yielding one to four usable channels; corrupted traces were flagged. Two-channel data sets were restricted to 1-1, 1-3, 11-1, 23-3, 33-4, and 36-4 (control) plus 16-2 (IDA). Baseline incompleteness affected 1-1, 7-1, 13-2, 20-3 (control) and 32-4 (IDA). Spontaneous activity was observed only in pregnant tissue following equilibration. Figure 8 illustrates representative screenshots from the same experiment in a pregnant control animal, while Figure 9 presents the corresponding BSL software screenshot from the IDA group.

Figure 8. Representative screenshot from the same experiment, recorded in a pregnant control group rat.

Figure 9. Representative screenshot from the same experiment, recorded in a pregnant IDA group rat.

Recording channels corresponded to parallel baths (e.g., “Banyo 1–4”). Processed signals were exported and all raw data were annotated with metadata. Only non-stimulated recordings—passive tension phases—were analyzed to address the primary aim of evaluating iron deficiency’s impact on baseline uterine tone. Signal conditioning included zeroing, 10 Hz low-pass filtering, and peak detection (≥0.05–0.10 g, ≥5 s spacing). All events were verified by manual inspection. All metrics were exported along with quantitative outputs included resting tone (mg), peak force (mg), contraction frequency, and mean peak-to-peak amplitude. These measurements constitute core biomechanical indices of myometrial function, encompassing both passive compliance and intrinsic rhythmic contractility (AUC, amplitude, frequency) (88).

Minimum and maximum values delineate the tension boundaries, with the maximum capturing peak contractile force. Mean values quantify average tone, while standard deviation characterizes variability across the recording window. Baseline drift denotes the cumulative change in baseline tone, and slope expresses this drift normalized over time (per second). Contraction frequency is assessed as events per minute, and intervals represent peak-to-peak timing, summarized by the mean interval.

The AUC computed relative to baseline (95), reflects total contractile effort and offers robustness compared to amplitude-only metrics. Recent work increasingly adopts AUC and peak contractile force as standard indicators of uterine function. For instance, (88) recorded myometrial contractions over 30–60 minutes in obese dams, extracting amplitude, frequency, and AUC before and after oxytocin and prostaglandin challenge. Each dataset was subjected to feature extraction to quantify mechanical tone and contractile behavior.

Contractility metrics were quantitatively defined: (i) baseline passive tension—the mean force over a contraction-free 60-second period post-equilibration; for continuous activity, the lowest stable inter-burst plateau of ≥30 s was used with linear detrending (≤0.1 g/10 min with Region 0; SC = Mean). (ii) Peak contractile force—maximum amplitude from baseline during a 10-minute window (Region 1; SC = Max). Here, the AUC was calculated via trapezoidal integration of tension above baseline over 600 seconds, while latency to first contraction was defined as time to first signal deflection >2 SD above baseline. (iii) Contraction frequency and amplitude—for spontaneously contracting strips, frequency was baseline, events/min above 0.1 g prominence; amplitude was calculated peak-to-peak (SC = I-MA). Latency to initial contraction, operationalized as the first deflection exceeding baseline by 2 SD, was extracted using the ΔT cursor.

3.10. Procedure for Evaluating Uterine Tension Recordings

To assess each channel's behavior, this thesis used key physiological phases in the tension recordings and implemented a strategy to detect and segment them automatically into five stages (Figure 10): (i) initial adjustment phase; (ii) equilibrated baseline phase (stable resting tone); (iii) onset of spontaneous contractions; (iv) sustained rhythmic contraction phase; and (v) final pre-stimulus phase.

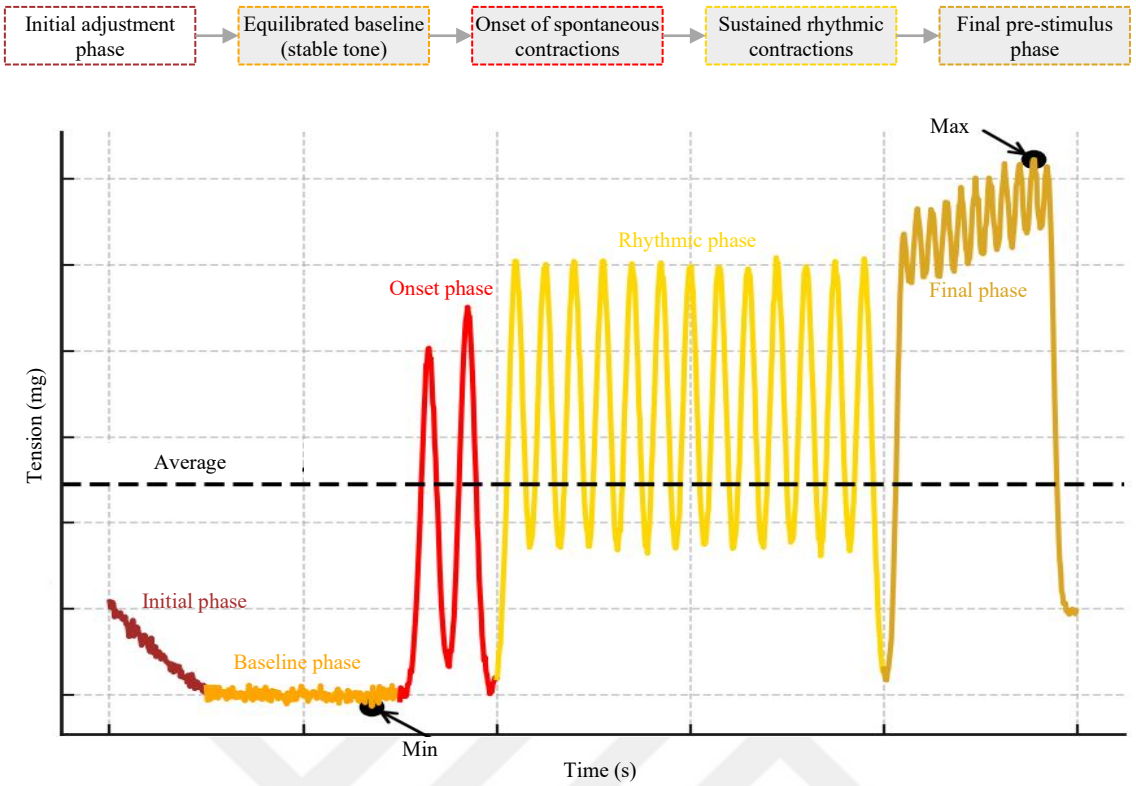

Figure 10. Singal stages observed in uterine tension recordings in BSL Analysis.

Upon mounting, the myometrial strip undergoes an adaptation period characterized by monotonic baseline drift under passive load and an absence of contractions.

- **Initial adjustment phase**: Right after mounting the tissue, the trace often shows a drift as the strip adapts to the set resting tension. This phase is characterized by a monotonic trend (tension either falls or rises toward a stable value) with no contractions. This study detected the end of this phase by finding when the baseline trend flattens out.
- **Equilibrated baseline (stable resting tone)**: Once adjusted, the tissue maintains a relatively stable passive tension. This passive baseline phase is a flat segment with minimal slope and no large oscillations. This research identifies segments of more than 30 seconds with very low variance and no peaks as candidate baseline intervals.
- **Onset of spontaneous contractions**: Pregnant uterine strips often begin to display spontaneous phasic contractions after the equilibration phase, particularly in control diet samples. The onset is identified when periodic fluctuations first appear above a defined threshold. Algorithmically, this can be detected by monitoring the signal's variance or by locating the first significant peak that exceeds a predefined criterion (e.g., >5% of

baseline tension or several standard deviations above baseline noise). The time of this first peak marks the onset of contractions.

- **Sustained rhythmic contraction phase**: After onset, contractions often become regular in amplitude and frequency – the trace shows repeating cyclic rises and falls. We segment this as the period of stable rhythmic activity. This can be identified by consistent peak-to-peak intervals and amplitudes. If contractions intensify gradually, we may mark the start of this phase after a few cycles have stabilized. In plots, this phase spans from the first consistent contraction onward until any external intervention.
- **Final phase (pre-stimulus end)**: Immediately before the application of an external stimulus or the termination of the recording, the trace may show a change in contraction patterns such as a final quiescent period or the continuation of rhythmic activity. The boundary of this phase is defined at the point where the recording transitions to stimulus application or stops. For recordings involving stimuli, this phase corresponds to the last 1–2 minutes of baseline activity before stimulation. If no stimulus was applied, the final phase extends to the end of the spontaneous activity record.

4. RESULTS

This study investigated the impact of maternal IDA on the biomechanics of the rat myometrium in late pregnancy. The objective was to determine how IDA alters the resting uterine tone (baseline passive tension) and the spontaneous contractility of longitudinal myometrial strips. Strips from IDA diet rats and IDA control rats (late gestation) were mounted in organ baths for resting tension recording. All samples were subjected to the same ex vivo protocol comprising five sequential phases: Initial (equilibration), baseline (resting tension), onset (beginning of spontaneous activity), rhythmic (established spontaneous contractions), and final (post-stimulation/end of experiment).

4.1. Measurement Metrics

Key mechanical metrics were computed for each phase, including mean baseline force, contraction peak force, contraction frequency, contraction latency (time to first contraction), and the area under the AUC over 600 s (an indicator of total contractile work). In this study, AUC was computed using two complementary approaches. First, raw AUC was derived by trapezoidal integration of the tension trace sampled at constant frequency ($\Delta t = 1/fs$). Second, a baseline-corrected AUC was calculated by estimating a linear baseline from the median values of the first and last 10 % of the trace, subtracting this baseline pointwise, and then applying trapezoidal integration. Contraction frequency (contractions·min^{-1}) was obtained by counting local maxima above a threshold defined as median + 0.5 of standard deviation, normalized by recording duration. Baseline drift was measured as the difference between the medians of the last and first 10 % of the signal. The global trend (slope, units·s^{-1}) was estimated via linear regression of tension versus time. For instantaneous trends, the notebook implementation applied a Savitzky–Golay filter, computing the numerical gradient; however, a global slope was reported as a scalar summary to ensure reproducibility in spreadsheets. All analyses were performed both with the BSL software and independently validated in Python (Google Colab environment) using NumPy for vectorized trapezoidal integration, with SciPy and scikit-learn libraries; GPU acceleration was unnecessary.

4.2. Functional Metrics from Pregnant Rats in Experimental Groups

In conducted trials, multiple myometrial strips were recorded simultaneously in two to three organ baths, often representing distinct dietary groups. This approach facilitated parallel data acquisition, with resulting files containing two or three channels. Among the 36 experiments, 6-1, 7-1, 16-2, 23-3, 31-4, and 32-4 belonged to the IDA group; the remainder were from the control diet group. Incomplete baseline data, caused by premature termination or calibration error, were noted in experiments. After equilibration, spontaneous contractile activity was evaluated to characterize intrinsic myometrial behavior without pharmacologic stimulation. Measurable contractions were observed almost exclusively in pregnant specimens.

4.2.1. Control Groups

Table 3 summarizes functional metrics from pregnant rats in the control group.

Table 3. Functional metrics from pregnant rats in control groups.

ID	Channel	Phase	Avg. Tension	Max	Baseline Drift	Slope	Freq.	|AUC|
C1	B 3	Baseline	411.63	456.04	23.03	0.41	0.00	878.36
C1	B 3	Rhythmic	419.10	485.65	1.64	0.00	0.00	9926.03
C2	B 3	Baseline	1825.42	10493.70	6142.99	0.75	0.00	48831298.67
C2	B 3	Rhythmic	5428.42	11054.50	2397.99	0.00	0.00	3694267.98
C2	B 4	Baseline	1003.46	5008.90	1698.46	0.47	0.00	17034356.55
C2	B 4	Rhythmic			0.00	0.00	0.00	0.00
C3	B 4	Baseline	1608.65	5264.16	2475.46	0.45	0.00	44708881.78
C3	B 4	Rhythmic			0.00	0.00	0.00	0.00
C4	B 3	Baseline	423.12	1543.19	1.64	0.00	0.00	3157363.05
C4	B 3	Rhythmic			0.00	0.00	0.00	0.00
C4	B 4	Baseline	1007.32	5008.90	1684.43	0.47	0.00	16948727.31
C4	B 4	Rhythmic			0.00	0.00	0.00	0.00
C5	B 3	Baseline	361.42	796.50	14.80	0.05	0.00	230179.35
C5	B 3	Rhythmic	2277.42	59900.80	864.30	0.00	0.00	52195990.20
C5	B 4	Baseline	29.29	153.35	39.27	0.49	0.00	54376.61
C5	B 4	Rhythmic	36.53	295.01	8.42	0.67	28.78	56809.81

C6	B 4	Baseline	1204.73	2794.31	116.41	0.11	0.00	727237.33
C6	B 4	Rhythmic	1309.23	7503.99	2430.58	2.72	3.36	102181845.56
C7	B 3	Baseline	758.58	5041.49	21.38	0.00	0.00	842650.37
C7	B 3	Rhythmic	2324.74	6844.09	5254.02	4.96	0.06	5003805.70
C7	B 4	Baseline	3139.53	13066.40	10840.16	10.85	0.00	28152768.32
C7	B 4	Rhythmic			0.00	0.00	0.00	0.00
C8	B 3	Baseline	758.39	5041.49	19.74	0.00	0.00	839949.98
C8	B 3	Rhythmic	2327.56	6844.09	5263.07	6.37	0.07	5096381.24
C8	B 4	Baseline	3145.45	13066.40	10837.36	13.89	0.00	28304508.63
C8	B 4	Rhythmic			0.00	0.00	0.00	0.00
C9	B 4	Baseline	623.20	2236.10	847.13	0.00	0.00	2019078.63
C9	B 4	Rhythmic	1257.49	4342.70	3172.51	0.35	0.19	15313108.16
C10	B 2	Baseline	5485.23	6667.91	75.09	0.00	0.00	96647.49
C10	B 2	Rhythmic	5059.02	7555.24	461.87	6.33	6.58	1054106.84
C10	B 3	Baseline	719.26	2959.29	97.04	0.00	0.00	52684.74
C10	B 3	Rhythmic	2313.99	6668.11	5179.19	0.00	0.00	982103.93
C10	B 4	Baseline	887.28	1596.55	297.34	0.00	0.00	19899.03
C10	B 4	Rhythmic			0.00	0.00	0.00	0.00
C11	B 2	Baseline	4642.77	4666.85	9.67	2.15	0.00	233.91
C11	B 2	Rhythmic	4646.14	4671.40	41.53	3.99	11.54	5.63
C11	B 3	Baseline	312.17	326.11	7.40	1.23	0.00	110.29
C11	B 3	Rhythmic	312.73	344.20	12.34	2.80	13.64	73.18
C11	B 4	Baseline	383.43	398.80	3.51	0.58	0.00	67.56
C11	B 4	Rhythmic	392.29	414.22	8.42	0.95	13.48	237.93
C12	B 3	Baseline	388.44	460.98	28.78	0.00	0.00	29722.59
C12	B 3	Rhythmic	1710.22	75056.80	2455.55	0.00	0.00	10080290.87
C12	B 4	Baseline	559.18	722.78	98.18	0.27	0.00	8887.50
C12	B 4	Rhythmic	1635.23	58739.70	2482.47	0.00	0.00	4490732.87
C13	B 3	Baseline	367.32	436.31	19.74	0.26	0.00	7427.36
C13	B 3	Rhythmic	374.00	1008.66	13.16	0.00	0.00	288727.11
C13	B 4	Baseline	94.73	290.80	78.54	0.00	0.00	9562.97
C13	B 4	Rhythmic	91.71	644.24	5.61	0.12	42.70	146722.74
C14	B 2	Baseline	5785.34	8011.43	882.22	0.00	0.00	10427722.18
C14	B 2	Rhythmic	6023.31	11038.60	565.96	0.00	0.00	1884164.72
C14	B 3	Baseline	296.19	1738.91	92.10	0.00	0.00	145255.10
C14	B 3	Rhythmic	2189.30	29787.80	574.00	0.00	0.00	94793180.89
C14	B 4	Baseline	3919.37	7696.14	678.83	0.00	0.00	35581020.79

C14	B 4	Rhythmic	2457.75	13790.10	3597.48	0.00	0.00	311891.46
C15	B 2	Baseline	22793.61	23969.80	1403.80	1.84	0.00	3939374.79
C15	B 2	Rhythmic			0.00	0.00	0.00	0.00
C15	B 3	Baseline	771.15	4870.44	1029.58	2.11	0.00	2463390.38
C15	B 3	Rhythmic	1506.75	8171.37	136.51	0.52	0.46	204598538.07
C15	B 4	Baseline	135.67	1445.08	2.81	0.00	0.00	1561862.73
C15	B 4	Rhythmic	1136.64	3513.81	542.78	0.96	16.62	10463957.07
C16	B 2	Baseline	5485.58	6667.91	85.33	28.44	0.00	91098.60
C16	B 2	Rhythmic	5059.47	7555.24	461.87	5.08	5.28	1052508.74
C16	B 3	Baseline	719.29	2959.29	97.04	2.60	0.00	51410.04
C16	B 3	Rhythmic	2316.72	6668.11	5182.48	0.00	0.00	886576.30
C16	B 4	Baseline	886.22	1596.55	294.53	9.41	0.00	23036.37
C16	B 4	Rhythmic			0.00	0.00	0.00	0.00
C17	B 2	Baseline	4642.77	4666.85	9.67	2.15	0.00	233.91
C17	B 2	Rhythmic	4646.14	4671.40	41.53	3.99	11.54	5.63
C17	B 3	Baseline	312.17	326.11	7.40	1.23	0.00	110.29
C17	B 3	Rhythmic	312.73	344.20	12.34	2.80	13.64	73.18
C17	B 4	Baseline	383.43	398.80	3.51	0.58	0.00	67.56
C17	B 4	Rhythmic	392.29	414.22	8.42	0.95	13.48	237.93
C18	B 3	Baseline	385.92	460.98	134.87	0.00	0.00	9327.86
C18	B 3	Rhythmic	1711.13	75056.80	2457.20	0.00	0.00	9995833.80
C18	B 4	Baseline	560.83	722.78	100.98	0.32	0.00	5233.49
C18	B 4	Rhythmic	1636.10	58739.70	2483.88	0.00	0.00	4416535.58
C18	B 3	Baseline	368.90	436.31	1.64	0.02	0.00	2942.42
C18	B 3	Rhythmic	374.00	1008.66	13.16	0.00	0.00	288727.11
C18	B 4	Baseline	69.66	243.11	11.22	0.00	0.00	11490.41
C18	B 4	Rhythmic	91.71	644.24	5.61	0.12	42.70	146722.74
C19	B 2	Baseline	5806.83	8011.43	931.70	0.00	0.00	10139195.02
C19	B 2	Rhythmic	6029.74	11038.60	774.15	0.00	0.00	1872269.70
C19	B 3	Baseline	301.07	1738.91	14.80	0.00	0.00	36291.97
C19	B 3	Rhythmic	2172.09	29787.80	580.59	0.00	0.00	94812645.72
C19	B 4	Baseline	4044.45	7696.14	645.15	0.00	0.00	35611836.64
C19	B 4	Rhythmic	2446.90	13790.10	3621.32	0.00	0.00	317567.54
C20	B 2	Baseline	22795.02	23969.80	1403.80	1.66	0.00	3943352.58
C20	B 2	Rhythmic			0.00	0.00	0.00	0.00
C20	B 3	Baseline	772.16	4870.44	1029.58	2.15	0.00	2465935.82
C20	B 3	Rhythmic	1507.20	8171.37	138.16	0.39	0.34	204579029.93

C20	B 4	Baseline	135.67	1445.08	4.21	0.01	0.00	1564598.20
C20	B 4	Rhythmic	1138.19	3513.81	539.97	0.83	14.31	10440774.81
C21	B 3	Baseline	422.76	460.98	45.23	0.00	0.00	7932.99
C21	B 3	Rhythmic	1400.18	8454.26	416.11	0.00	0.00	34560402.81
C21	B 4	Baseline	370.63	414.22	42.78	0.00	0.00	16932.26
C21	B 4	Rhythmic			0.00	0.00	0.00	0.00
C22	B 3	Baseline	1825.22	10493.70	6142.17	0.76	0.00	48828469.05
C22	B 3	Rhythmic	5562.81	11054.50	370.06	0.00	0.00	13790611.90
C22	B 4	Baseline	1000.31	5008.90	1638.15	0.74	0.00	17523515.77
C22	B 4	Rhythmic			0.00	0.00	0.00	0.00
C22	B 4	Baseline	1613.33	5264.16	2522.45	0.69	0.00	46107614.36
C22	B 4	Rhythmic			0.00	0.00	0.00	0.00
C23	B 3	Baseline	1825.02	10493.70	6141.34	0.75	0.00	48821432.58
C23	B 3	Rhythmic	5540.98	11054.50	787.82	0.00	0.00	9693077.00
C23	B 4	Baseline	995.73	5008.90	1562.42	0.34	0.00	10950611.25
C23	B 4	Rhythmic			0.00	0.00	0.00	0.00
C24	B 3	Baseline	361.53	796.50	11.51	0.07	0.00	216550.58
C24	B 3	Rhythmic	2282.15	59900.80	1038.63	0.50	2.95	42385601.96
C24	B 4	Baseline	30.86	147.74	37.87	0.00	0.00	67119.26
C24	B 4	Rhythmic	8.83	2574.11	49.09	0.02	2.76	1325921.59
C25	B 4	Baseline	1205.03	2794.31	186.53	0.17	0.00	788273.77
C25	B 4	Rhythmic	1311.01	7503.99	2473.35	3.14	3.81	102254610.42
C26	B 3	Baseline	758.39	5041.49	19.74	0.00	0.00	839949.98
C26	B 3	Rhythmic	2327.56	6844.09	5263.07	6.37	0.07	5096381.24
C26	B 4	Baseline	3145.45	13066.40	10837.36	13.89	0.00	28304508.63
C26	B 4	Rhythmic			0.00	0.00	0.00	0.00
C26	B 3	Baseline	758.25	5041.49	18.09	0.00	0.00	838219.46
C26	B 3	Rhythmic	2330.21	6844.09	5268.01	7.30	0.08	5117470.85
C26	B 4	Baseline	3150.25	13066.40	10786.86	15.75	0.00	28283465.35
C26	B 4	Rhythmic			0.00	0.00	0.00	0.00
C27	B 4	Baseline	628.13	2236.10	833.10	0.00	0.00	2123438.72
C27	B 4	Rhythmic	1255.62	4342.70	3162.69	0.35	0.18	15231859.63

The control group exhibited wide variability in spontaneous activity. Several channels displayed very high rhythmic AUC values, consistent with robust phasic contractions and the development of active tone characteristic of late pregnancy. However, mismatches

between large AUC and zero reported frequency highlighted incomplete baseline data, often due to premature termination or calibration errors. Overall, as presented in Table 3, control strips could generate substantial spontaneous work output.

4.2.2. IDA Group

Table 4 presents corresponding metrics from pregnant rats in the IDA group. AUC in the rhythmic phase served as the main metric, representing contractile work. Average tension (mg) and frequency (events/600 s) were also assessed in baseline and rhythmic phases. As shown in Tables 3 and 4, occasional malfunctions of force transducers reduced the number of functional channels to two or fewer; such events were documented without substitution. Recordings therefore ranged from one to four active channels, with inactive or artifact contaminated traces flagged. Specifically, experiments were restricted to two channels because of transducer failure.

Table 4. Functional metrics from pregnant rats in IDA pregnant group.

ID	Channel	Phase	Avg. Tension	Max	Baseline Drift	Slope	Frequency	|AUC|
D1	B 3	Baseline	730.08	2085.95	539.47	2.17	0.00	154391.26
D1	B 3	Rhythmic	747.35	4092.49	54.28	0.00	0.00	1494350.70
D1	B 4	Baseline	1366.71	7177.21	6413.06	6.54	0.00	7841381.16
D1	B 4	Rhythmic			0.00	0.00	0.00	0.00
D2	B 3	Baseline	426.16	472.49	37.83	0.64	0.00	3509.73
D2	B 3	Rhythmic	437.27	849.13	0.00	0.00	0.00	1226860.57
D2	B 4	Baseline	19.10	105.67	33.66	0.48	0.00	18108.20
D2	B 4	Rhythmic			0.00	0.00	0.00	0.00
D3	B 3	Baseline	358.48	403.41	39.47	6.94	0.00	2078.85
D3	B 3	Rhythmic	1558.92	11648.30	1620.04	0.66	131.22	1724548.75
D4	B 3	Baseline	355.71	403.41	27.14	2.98	0.00	1195.80
D4	B 3	Rhythmic	1558.76	11648.30	1618.39	0.57	113.06	1993680.84
D5	B 3	Baseline	730.29	2085.95	552.62	2.09	0.00	151049.54
D5	B 3	Rhythmic	747.51	4240.52	54.28	0.00	0.00	1509763.89
D5	B 4	Baseline	1426.83	7177.21	6529.46	6.56	0.00	7367467.43
D5	B 4	Rhythmic			0.00	0.00	0.00	0.00
D6	B 3	Baseline	426.16	472.49	37.83	0.64	0.00	3509.73
D6	B 3	Rhythmic	437.27	849.13	0.00	0.00	0.00	1226860.57
D6	B 4	Baseline	19.10	105.67	33.66	0.48	0.00	18108.20
D6	B 4	Rhythmic			0.00	0.00	0.00	0.00

As shown in Tables 3 and 4, occasional malfunctions of force transducers reduced the number of functional channels to two or fewer; such events were documented without substitution. Recordings therefore ranged from one to four active channels, with inactive or artifact contaminated traces flagged. Specifically, experiments were restricted to two channels because of transducer failure.

5. DISCUSSIONS

5.1. Comparison of Absolute AUC Through Different Phases Between Control and IDA Groups in All Samples

Figure 11 summarizes the observed absolute latency, AUC, frequency, and average tension to the first spontaneous contraction among all experimental samples in all observed bath channels.

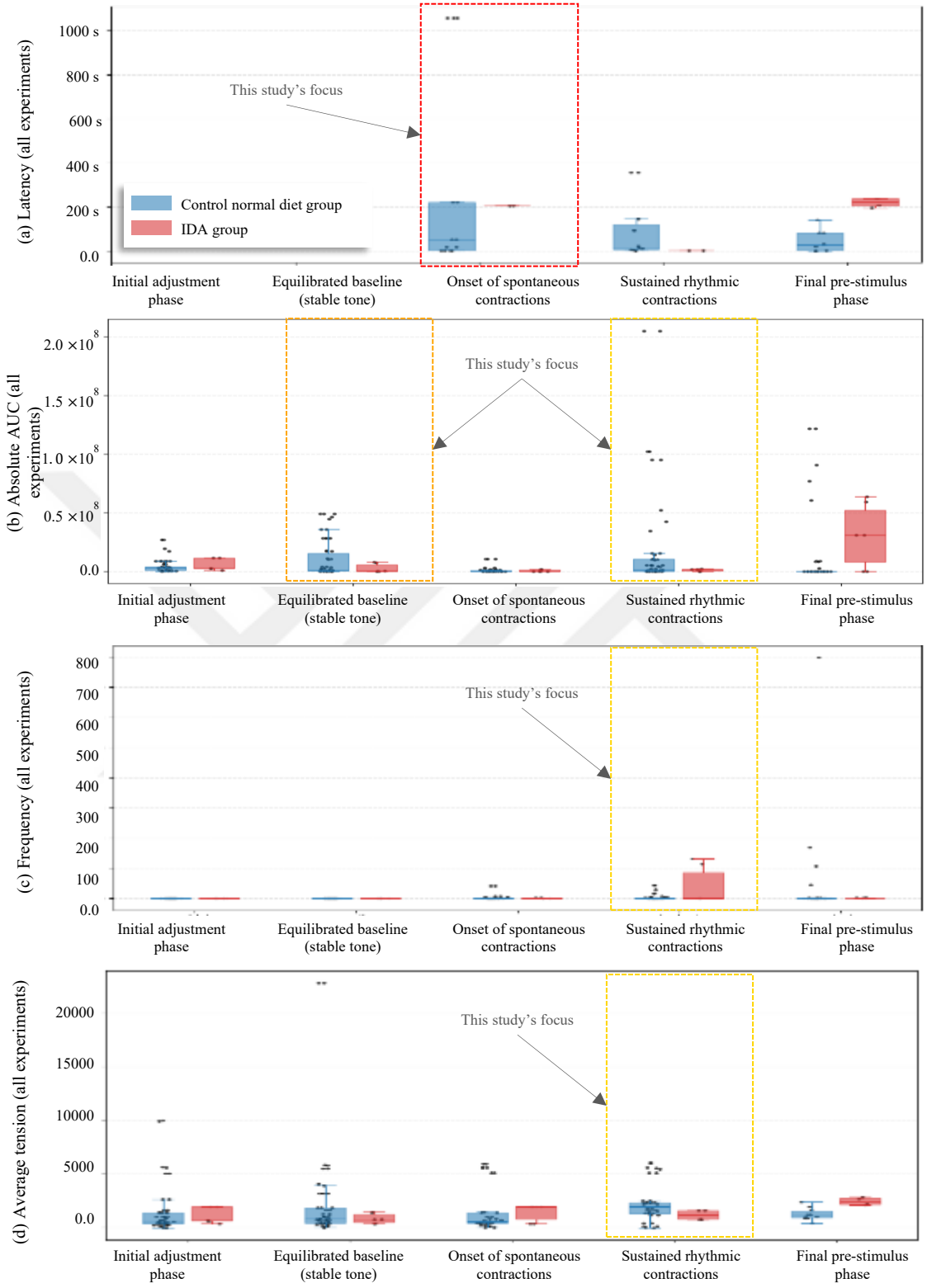

Figure 11. Comparison of absolute AUC between the control and IDA by experimental phases in all samples.

As illustrated in Figure 11a, control samples predominantly initiate rhythmic activity within about 1–3 minutes during the rhythmic phase. IDA displays a bimodal pattern: many strips show no spontaneous contraction, while a minority exhibit near zero latencies due to tiny, rapidly recurring twitches. This pattern highlights that latency alone is a poor discriminator without concurrent amplitude and integral context of AUC.

Moreover, as indicated in Figure 11b, AUC diverges strongly by group only in the rhythmic phase: controls cluster high with wide but consistently elevated AUC, whereas IDA samples are compressed near the axis (very low AUC). Early phases (initial, baseline, onset) show similarly low AUC in both groups, indicating the group effect is phase specific (spontaneous activity).

5.2. Comparison of Tension through Baseline and Rhythmic Phases Between Control and IDA Groups in All Samples

Figure 12 shows average tension observed values through baseline and rhythmic Phases across experimental samples.

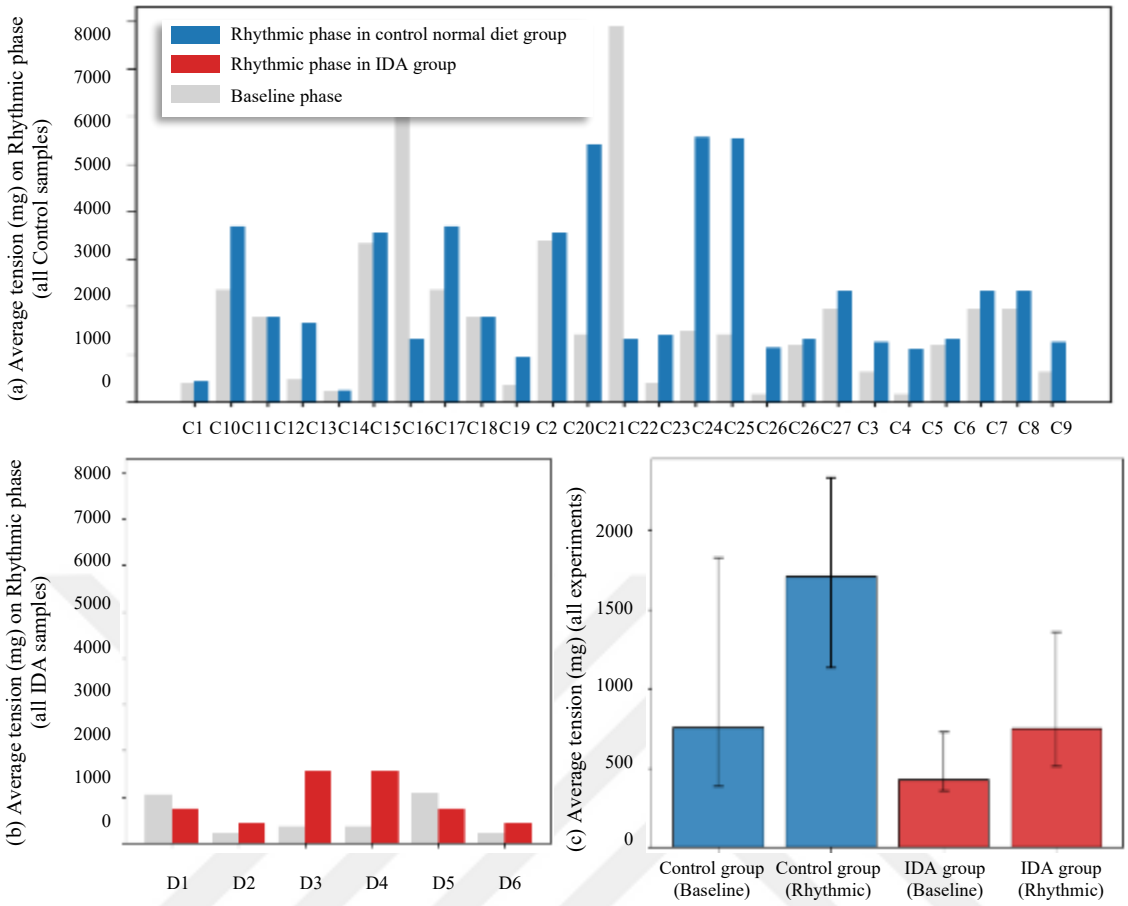

Figure 12. Average tension values across all experimental strips during baseline and rhythmic phases.

Across all strips, average tension showed clear phase- and group-specific patterns (Figure 12). In Controls, tension rose consistently from baseline to rhythmic, indicating the recruitment of active tone as spontaneous phasic contractions became established. In IDA, this increase was attenuated or absent, with several strips remaining close to baseline despite entering the rhythmic period. By contrast, IDA strips showed little change. Between groups in the rhythmic phase, average tension was lower in IDA.

Physiologically, this thesis suggests iron deficiency restricts the transition from passive baseline to sustained active force during spontaneous activity. Such blunting is consistent with defects in excitation–contraction coupling or impaired energy availability, leaving IDA strips unable to sustain cross-bridge cycling. As a result, IDA uteri exhibit preserved baseline tension but lack the robust elevation seen in Controls, contributing to reduced contractile work.

5.3. Comparison of Absolute AUC through Baseline and Rhythmic Phases Between Control and IDA Groups in All Samples

Figure 13 shows absolute AUC values through baseline and rhythmic Phases across experimental samples.

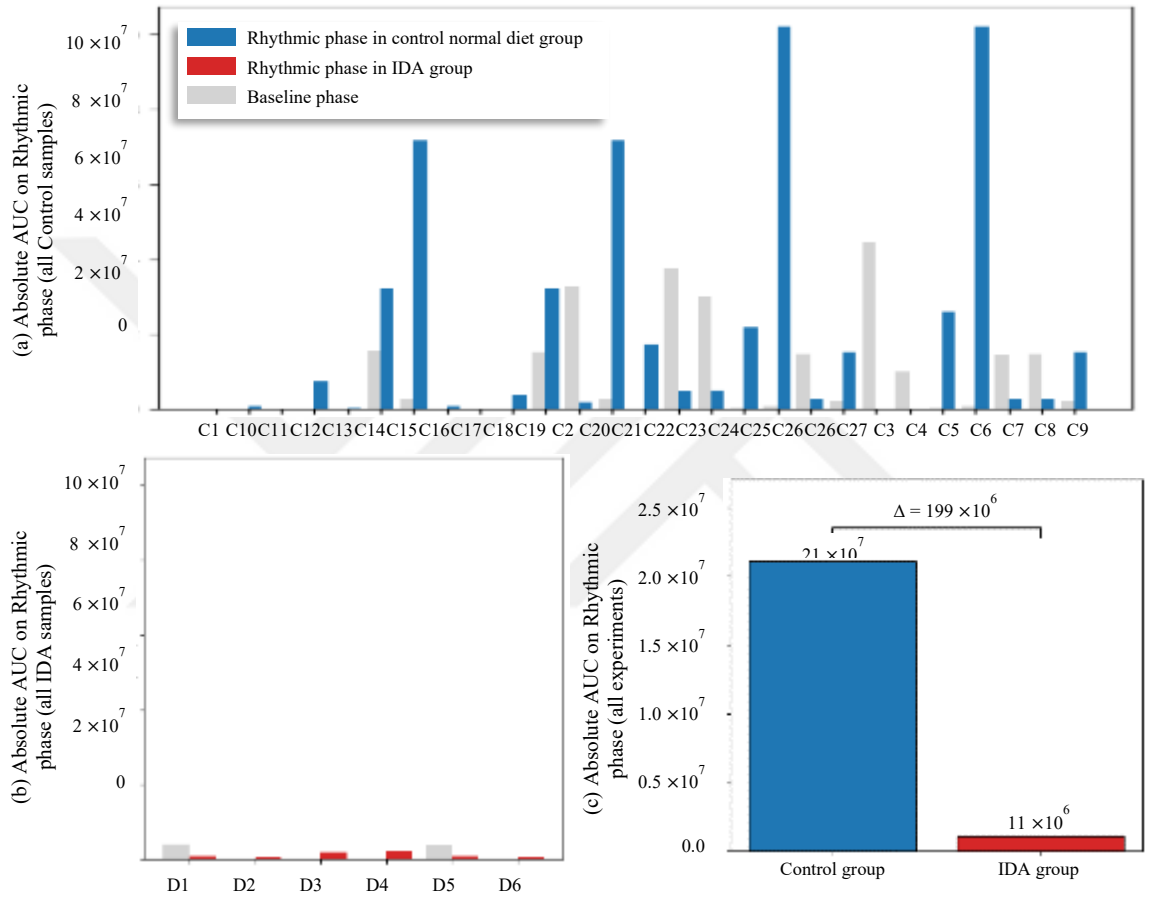

Figure 13. Absolute AUC values across baseline and rhythmic phases in experimental samples.

As observed from Figures 13a and 13b, baseline AUC was uniformly low in both cohorts, indicating comparable quiescent tone. In contrast, during the rhythmic phase, Control channels displayed consistently elevated and widely distributed AUC values, while IDA channels clustered near zero, with only a few modest responders. This pattern demonstrates that group differences arose from reduced spontaneous phasic activity under iron deficiency rather than altered baseline tone.

Figure 13c further illustrates the substantial group disparity in spontaneous contractility of rhythmic phase AUC and contraction frequency between the Control and IDA samples. Findings highlight the pronounced disparity in spontaneous contractility between Control and IDA groups. Control samples produced an average rhythmic phase AUC of 21×10^7 units, whereas IDA samples yielded only 11×10^6 units, reflecting a very large effect size. Contraction frequency followed a similar pattern: Controls averaged 24 contractions per 600 s, compared to just 4.1 events in IDA ($\Delta = 19.9$). These results confirm that maternal IDA severely reduces both the amplitude and temporal regularity of spontaneous myometrial activity. Together, the findings reinforce that IDA impairs uterine excitability and force generation, consistent with a defect in excitation–contraction coupling. Despite the limited IDA sample size, these contrasts remained robust due to strict data quality criteria minimizing artifacts.

5.4. Comparison of Frequency through Baseline and Rhythmic Phases Between Control and IDA Groups in All Samples

Figure 14 illustrates the variation in mean contraction frequency between the baseline and rhythmic phases across the analyzed samples.

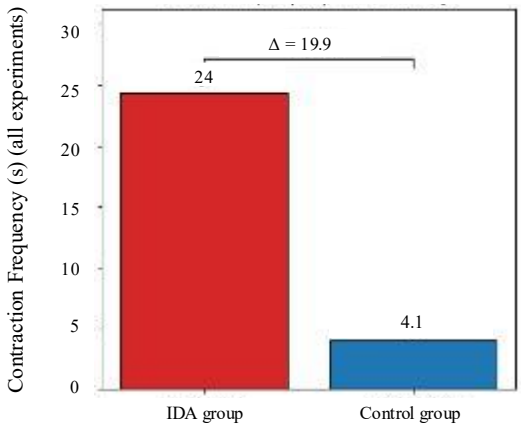

Figure 14. Average contraction frequency across baseline and rhythmic phases in experimental samples.

This thesis compares (Figure 14) average contraction frequency during the rhythmic phase between groups. IDA strips displayed a higher event count (24 events/600 s) than

Controls (4.1 events/600 s), a raw difference of $\Delta = 19.9$. While this appears to suggest heightened activity, the AUC and mean-tension results show that IDA contractions were typically small twitches or brief oscillations.

5.5. Channel Selection from Experimental Samples

As stated earlier, in the conducted trials, in some experiments, force transducer failure reduced active channels to two or fewer. These cases were recorded without substitution. Channels with artifacts or inactivity were excluded. Therefore, to better characterize group differences, we therefore focused on a subset of the most responsive preparations in each group for detailed analysis. In selecting the sample quality definition, the rhythmic phase segments were used to quantify spontaneous contractility. Quality was operationalized a priori as (i) presence of a complete rhythmic segment without acquisition artifacts; (ii) coherent contraction morphology; and (iii) a nonzero, internally consistent AUC signal reflecting integrated force production. For each recorded experiment, multiple channels were available from parallel organ baths. To avoid within experiment duplication while maximizing signal fidelity, the best single channel per sheet was chosen using the largest absolute AUC during the rhythmic phase as an objective proxy for signal strength and completeness. Figures 15 and 16 present representative sample recordings obtained from the control and IDA groups, respectively.

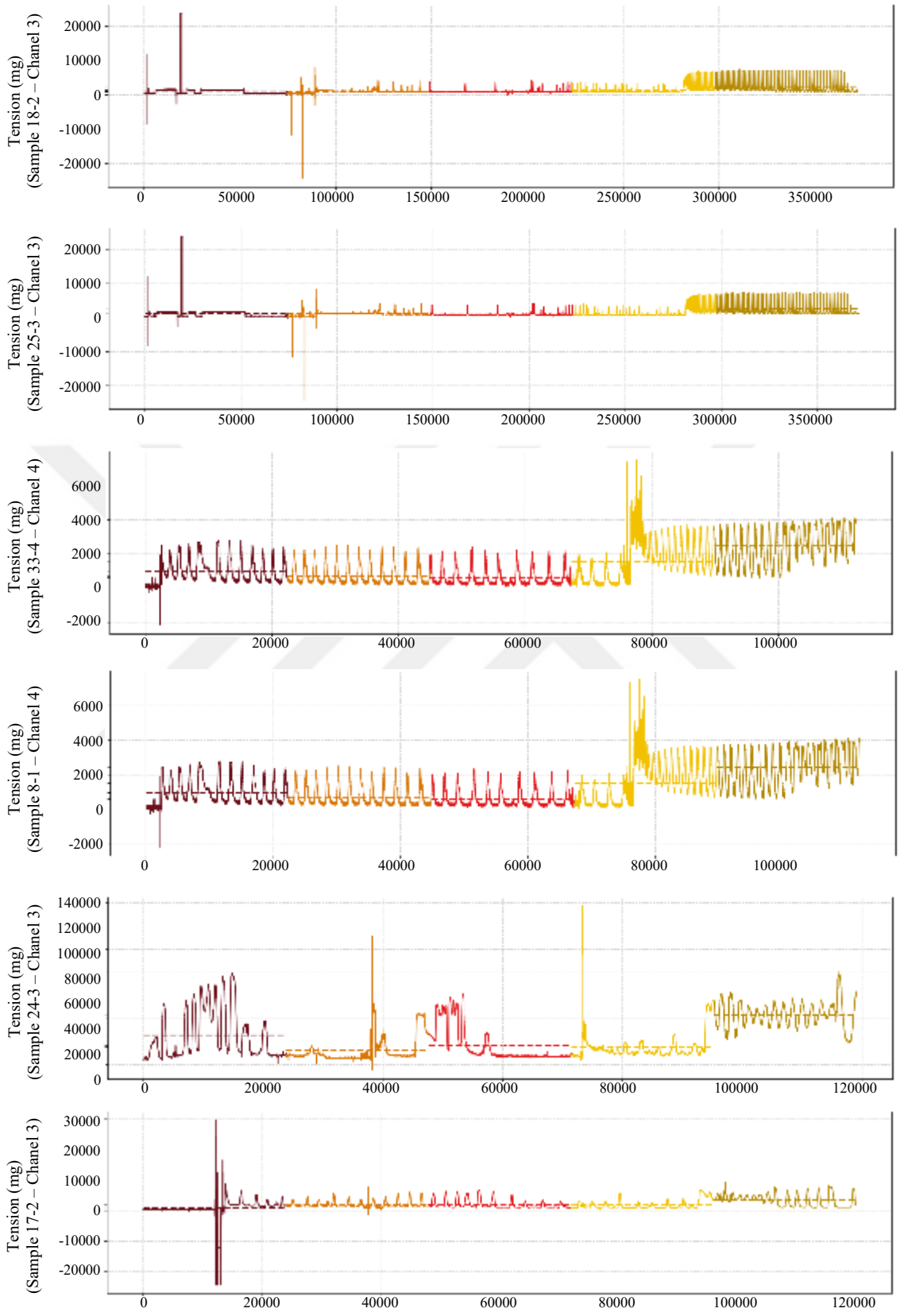

Figure 15. Experimental results of six selected samples from the control pregnant group.

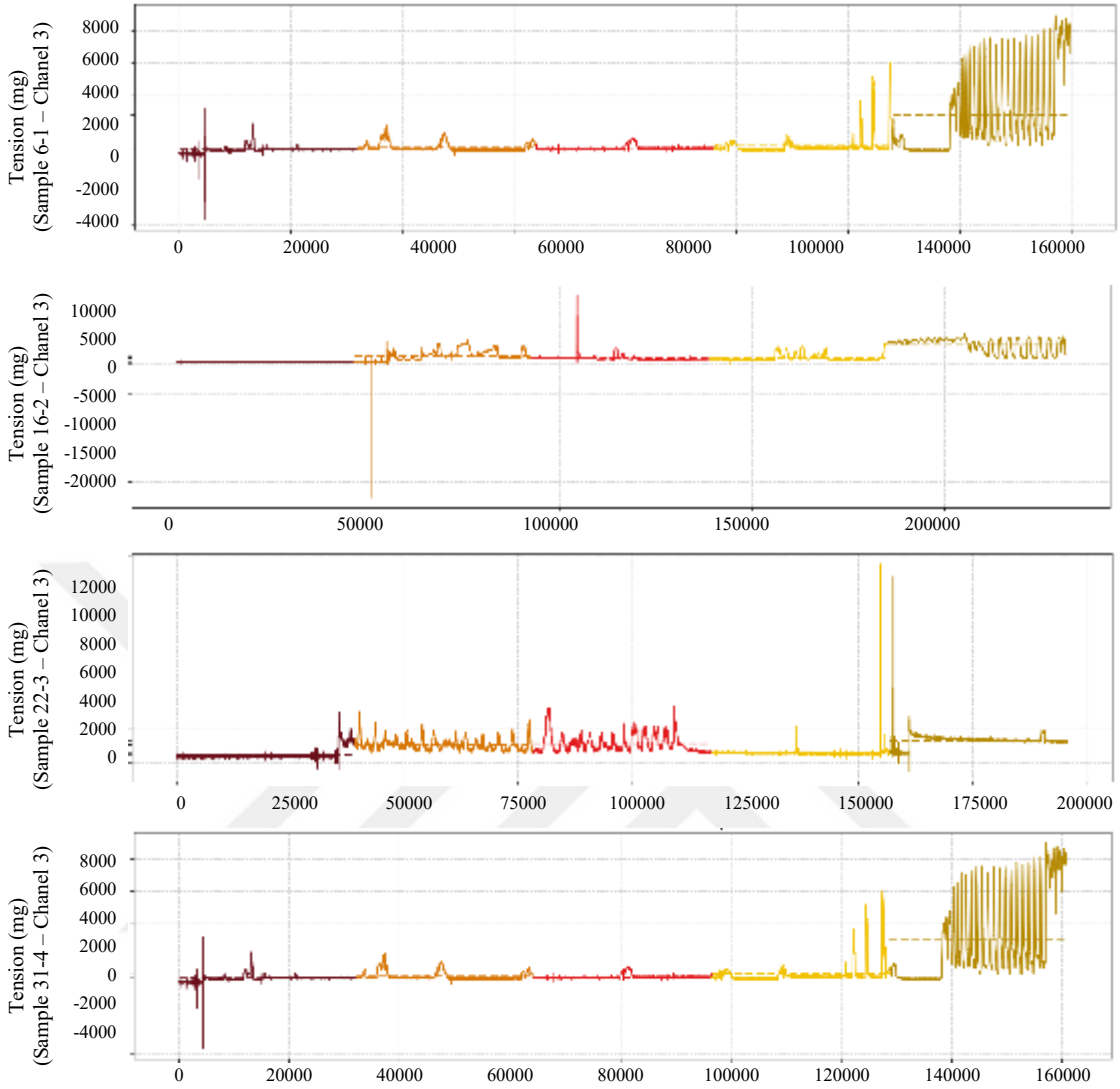

Figure 16. Experimental results of six selected samples from the IDA pregnant group.

5.6. Comparison of Absolute AUC Between Control and IDA Groups in Selected Samples

Figure 17. compares the AUC (integrated tension) in each phase, comparing Control vs IDA groups.

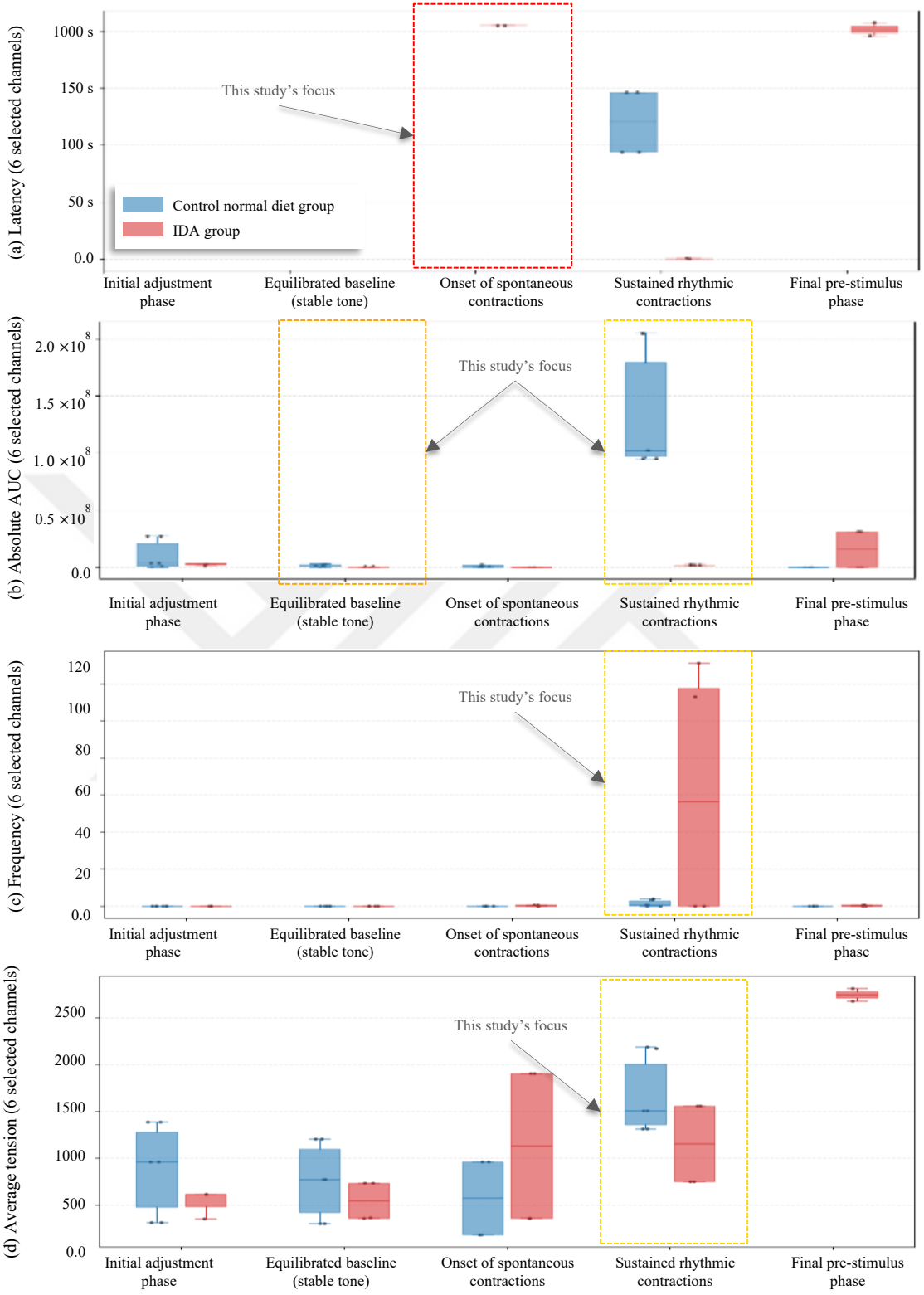

Figure 17. Comparison of absolute AUC between the control and IDA by experimental phases in six selected samples.

5.7. Statistical Analysis Approach

Given the characteristics of our data, a traditional two-way ANOVA and MANOVA (which could test for group × phase interactions) was not feasible. The contractility metrics showed strong skewness, outliers, and many zero values, violating assumptions of normality and homoscedasticity. Additionally, the IDA group's small sample size (only 6 animals, with fewer strips yielding usable contractions) would make multi-factor models unstable. We therefore employed paired or independent non-parametric tests for most comparisons, using parametric t-tests only when assumptions were reasonably satisfied. This strategy ensured a robust analysis despite the data's non-normal distribution and unequal sample sizes.

Before each hypothesis test, normality was assessed with the Shapiro–Wilk test ($\alpha = 0.05$). For within-strip comparisons (baseline vs. rhythmic phase on the same strip), we evaluated the distribution of the paired differences. If the differences passed normality ($p > 0.05$), a paired t-test was used (reporting t, degrees of freedom, and p). If not, we used the Wilcoxon signed-rank test (reporting the sum of ranks W and p). For between-group comparisons (Control vs. IDA), we first tested each group's values for normality. If both groups were roughly normal and variances comparable, an independent-samples t-test (Welch's t if variances differed) was applied. Otherwise, we used the Mann–Whitney U test (reporting U and p). Non-parametric tests were conducted two-tailed. Alongside significance, we report effect sizes: Cohen's z for paired t-tests (where 0.2 is small, 0.5 medium, 0.8 large), rank-biserial r for Wilcoxon tests (range –1 to +1, where +0.5 is a medium-large increase), Hedges' g for two-sample t-tests (bias-corrected d), and Cliff's δ for Mann–Whitney tests ($\delta = \pm 1$ indicates no overlap between groups). All analyses were performed using standard statistical software and cross-checked with custom Python scripts (NumPy/SciPy). Significance was set at $\alpha = 0.05$ (exact p-values are given, in scientific notation when very small). This analytical approach balances rigor and practicality, given the dataset's limitations, and forms the basis for the results presented in the next sections.

5.8. Within-Group Changes from Baseline to Rhythmic Phase

This thesis first examined how myometrial contractility shifted from the baseline period, reflecting resting tone, to the rhythmic phase, characterized by spontaneous

contractions, within each dietary group. The primary endpoints were integrated contractile work, expressed as |AUC| over 600 s, and mean tension.

5.8.1. Control Group

This thesis found that late-pregnant, IDA rats displayed a pronounced increase in uterine activity from baseline to rhythmic phases. In paired strip analyses, the absolute AUC rose markedly during the rhythmic phase. Because the distribution of AUC differences was highly non-normal (Shapiro–Wilk $p \ll 0.001$), the Wilcoxon signed-rank test was used, confirming a significant increase in contractile work ($W = 218.0$, $p = 0.0029$). The rank-biserial correlation was $r = +0.48$, a medium-to-large effect, indicating that ~75% of strips showed greater rhythmic than baseline AUC. Similarly, average isometric tension increased between phases. Here the differences were approximately normal (Shapiro–Wilk $p = 0.102$), supporting use of a paired t-test, which showed a significant effect ($t(33) = –4.554$, $p = 6.82\times10^{-5}$). The corresponding Cohen's z was –0.78, indicating a large effect, with rhythmic mean tension ~0.78 standard deviation higher than baseline. In summary, this study demonstrated that uterine strips from control rats had significantly greater contractile work and higher tone once spontaneous contractions were established.

5.8.2. IDA Group

This thesis observed that only a minority of strips from iron-deficient rats developed rhythmic contractions. Complete baseline–rhythmic data were available for 4 strips, as many IDA samples either lacked rhythmic activity or suffered recording issues. In these 4 strips, |AUC| during the rhythmic phase increased relative to baseline (which was essentially zero in all cases). The differences satisfied normality (Shapiro–Wilk $p = 0.333$), allowing use of a paired t-test. Despite the small sample, the increase was significant: $t(3) = –10.229$, $p = 0.0020$. Cohen's $z = –5.12$, an extremely large effect, reflecting the contrast between silent baseline traces and low but non-zero rhythmic AUC values. In contrast, mean tension changes were not significant. Tension differences appeared non-normal (Shapiro–Wilk $p = 0.024$), so Wilcoxon testing was applied, yielding $W = 0.0$, $p = 0.125$. The rank-biserial effect size was $r = +1.00$, showing all four strips had higher rhythmic than baseline tension, but this trend did not reach significance with such a small n. Overall, while some IDA strips

displayed measurable increases in contractility, many failed to contract, making the within-group effect difficult to demonstrate statistically. This outcome foreshadows the more pronounced between-group contrasts reported later.

5.9. Between-Group Comparison of Contractile Activity (All Samples)

This thesis next evaluated differences in uterine contractility between Control and IDA groups to test the impact of maternal iron deficiency. The primary outcome was the absolute AUC during the rhythmic phase, reflecting the total contractile work generated over 10 minutes of spontaneous activity. Secondary measures included contraction frequency and mean tension. To ensure unbiased assessment, all available strips were analyzed, including those with low-quality recordings or absent contractions.

5.9.1. Rhythmic AUC (All Strips)

In both groups, the distribution of rhythmic phase |AUC| was highly skewed. Many strips, especially in IDA, had near-zero values indicating absent contractions, while some control strips exhibited very high AUC due to strong contractility. Normality was strongly rejected ($p < 0.001$), so a Mann–Whitney U test was applied. The comparison showed no significant difference between Control and IDA ($U = 178.0$, $p = 0.459$). Practically, the overlap reflected high variability: both groups included inactive strips, although inactivity was more common in IDA. Similar results emerged for secondary metrics. Contraction frequency medians were 0 in both cohorts, as rhythmic contractions occurred only in a subset of controls. Mean tension during the rhythmic phase was also skewed and variable; a Mann–Whitney test found no significant group effect ($p > 0.3$). Thus, when all strips were included, IDA did not differ statistically from controls. Potential group differences were obscured by the abundance of non-contractile or poor-quality samples in both groups. Consistent with this, Chapter 4's findings shows divergence only in the rhythmic phase, where many IDA strips remain at zero while some control strips are also low.

5.9.2. Data Quality Consideration

Technical artifacts such as transducer failure and signal noise, together with biological variation such as inherently non-contractile strips, could conceal real effects. Therefore, in

line with the analysis plan, a targeted subset analysis was performed on the highest-quality strips. This allowed the question to be tested directly: under optimal conditions, does iron-deficient myometrium generate less contractile work than control tissue?

5.10. Focused Analysis on Strip Samples (Best Strips per Animal)

Table 5 summarizes the baseline mechanical and spontaneous contractility metrics for the top 6 control rat myometrial samples (selected for stable, high-quality recordings. Six representative control myometrial strips are shown with their baseline tension and spontaneous contraction parameters. Baseline tension is the resting force during the baseline phase. AUC is an integrated tension time area over 600 s of spontaneous contractions (reported in 10^6 $force \times seconds$ units for readability). Frequency is the number of spontaneous contractions per 600 s. Latency is the time from baseline to the first detected contraction. Skewness represents the asymmetry of tension distribution during the rhythmic phase. Values demonstrate the range among control samples, with relatively high baseline tone and robust spontaneous contractions.

Table 5. Baseline tone and spontaneous contraction metrics for six control late dam myometrial strips (highest quality recordings).

Control Sample	Baseline Tension (mg)	AUC (10^6 units)	Frequency (cycles/600 s)	Latency (s)	Skewness
1	771	204.6	0.5	94	2.6
2	772	204.6	0.3	94	2.6
3	1205	102.3	3.8	146	0.9
4	1205	102.2	3.4	146	0.9
5	301	94.8	0.0	6	3.5
6	296	94.8	0.0	6	3.4

As shown in the Table 5, the baseline tension shows the resting uterine tone prior to contractions, on the order of 0.3–1.2 g in these samples. Control strips developed substantial spontaneous contractile activity: the AUC (integrated force over 10 min) ranged from about 9.5×10^7 to 2.0×10^8 (arbitrary units), reflecting high overall contraction output. Most control samples generated multiple rhythmic contractions (frequency of 3–4/600 s in Samples 3–4), although some showed a single large contraction (Samples 1–2, frequency <1). The latency

to first contraction varied from nearly immediate (about 6 s in Samples 5–6) to around 1.5–2.5 minutes (Samples 1–4). Skewness values indicate that tension distributions were often right skewed (e.g. 2.6 in Samples 1–2), due to occasional high amplitude contractions on an otherwise lower baseline. Two samples (5–6) showed negative skewness (−3.4), suggesting a slight left tailed distribution (these had an initial high tension followed by a drop, possibly due to a single contraction causing a net tension decrease). Overall, control myometrial strips maintained a notable baseline tone and exhibited robust spontaneous phasic contractions.

Table 6 presents the corresponding data for 6 IDA rat samples. Six late dam myometrial strips are shown with the same metrics. These samples were chosen as the most reliable IDA recordings. The data reveals stark differences from controls, including lower baseline tension and greatly diminished spontaneous contractile activity in most cases.

Table 6. Baseline tone and spontaneous contraction metrics for six IDA myometrial strips.

IDA Sample	Baseline Tension (mg)	AUC (10^6 units)	Frequency (cycles/600 s)	Latency (s)	Skewness
1	356	1.99	113.1	0.5	1.1
2	358	1.72	131.2	0.4	1.1
3	730	1.51	0.0	19.7	6.2
4	730	1.49	0.0	19.7	6.1
5	426	1.23	0.0	30.5	0.5
6	426	1.23	0.0	30.5	0.5

All selected control strips (Table 5) exhibited robust spontaneous contractile activity, with rhythmic phase AUC values ranging from approximately 95 × 10^6 to 205 × 10^6, indicating substantial total force generation over the 10-minute observation period. In four of the six samples, multiple contractions were observed (with frequencies of approximately 3–4 events per 600 seconds), whereas Samples 1 and 2 displayed a single large contraction, resulting in frequencies below one per 10 minutes.

Baseline tension across these control strips varied between 0.3 g and 1.2 g, reflecting the intrinsic uterine tone prior to the onset of phasic activity. The latency to first contraction ranged from nearly immediate initiation (e.g., around 6 seconds in Samples 5 and 6) to

delayed onset (1.5 to 2.5 minutes in Samples 1–4), demonstrating inter-sample variability in excitation thresholds.

Analysis of tension skewness revealed generally positive values in most control strips. Samples 1 and 2 showed a skew of approximately +2.6, suggesting right-skewed distributions dominated by a single high-amplitude event. Samples 3 and 4 demonstrated more balanced skew values (~+0.9), consistent with multiple contractions and a more symmetrical force profile. Interestingly, Samples 5 and 6 presented negative skew values (–3.4 to –3.5)—an uncommon finding—likely due to a substantial post-contraction decline in baseline tension, resulting in a left-skewed profile relative to initial tone.

In stark contrast, even the highest-quality strips from the IDA group (Table 6) exhibited minimal contractile activity, with rhythmic phase AUC values ranging from approximately 1.2×10^6 to 2.0×10^6, representing a nearly 100-fold reduction compared to control samples. Four of the six strips (Samples 3–6) showed no discernible rhythmic contractions (frequency = 0), indicating either complete absence of spontaneous activity or only a single, barely detectable twitch within the 10-minute observation window. This was further reflected in their long contraction latencies (20–30 seconds or more) and minimal AUC values.

The remaining two IDA strips (Samples 1 and 2) presented with abnormally high contraction frequencies (exceeding 100 events per 600 seconds); however, these were characterized by very low-amplitude twitch-like events, contributing negligibly to total force output and leaving AUC values below 2×10^6.

Baseline tension in the IDA cohort was also lower on average (ranging from 0.35 to 0.73 g) compared to the control group, consistent with a reduction in intrinsic uterine tone. Skewness values in IDA strips were markedly elevated in samples with a single small spike (e.g., ~6.0 in Samples 3–4), indicative of an isolated event superimposed on an otherwise quiescent baseline. In contrast, strips lacking meaningful contractions displayed minimal skew (~0.5), suggestive of baseline noise without contractile events.

Collectively, these findings demonstrate a profound impairment in spontaneous myometrial activity in the IDA group, even under optimized experimental conditions. The inability to generate or sustain forceful contractions is consistent with a failure in excitation–contraction coupling or a deficit in energetic reserve within the iron-deficient uterine tissue.

5.11. Between-Group Comparison: Selected Sample Strips

To consolidate these findings, Table 7 summarizes the statistical tests applied to each primary metric, along with their results and effect sizes. This table summarizes statistical comparisons conducted in this study. Paired comparisons (rhythmic vs baseline) examine within-strip differences across contraction phases, while independent comparisons (Control vs IDA) assess group-level differences. Normality of data distributions or difference scores was evaluated using the Shapiro–Wilk test. Reported effect sizes include rank-biserial correlation (r) for Wilcoxon tests, Cohen's d_z for paired t-tests, and Cliff's delta (δ) for Mann–Whitney U tests. For the subset comparison of highest-quality strips between groups, Hedges' g was approximately 3.15—denoting a very large group difference, aligned with t-test results.

Table 7. Statistical comparisons across contraction phases and diet groups.

Comparison (Outcome)	Sample(s)	Normality	Test Used	Statistic	p-value	Effect Size
Control: Rhythmic vs Baseline (AUC)	34 paired strips	Non-normal Differences ($p < 0.0001$)	Wilcoxon Signed Rank	$W = 150.0$	0.0107	$r = +0.50$ (medium large)
Control: Rhythmic vs Baseline (Mean tension)	34 paired strips	Normal Differences ($p = 0.102$)	Paired *t*-test	$t(33) = -4.554$	6.8×10^{-5}	$dz = -0.78$
IDA: Rhythmic vs	4 paired stri	Normal Differences ($p = 0.333$)	Paired *t*-test	$t(3) = -10.229$	0.0020	$dz = -5.12$

Comparison (Outcome)	Sample(s)	Normality	Test Used	Statistic	p-value	Effect Size
Baseline (AUC)	ps					
IDA: Rhythmic vs Baseline (Mean tension)	4 paired strips	Non-normal differences (p = 0.024)	Wilcoxon signed-Rank	W = 0.0	0.125	r = +1.00 max, n.s.)
Control vs IDA: All Strips (Rhythmic AUC)	Control n=50, IDA n=6 (channels)	Non-normal (skewed)	Mann Whitney U	U = 178.0	0.459	δ = 0.21 (small)
Control vs IDA: Best strips (Rhythmic AUC)	Control n=6, IDA n=6	Non-normal (Control p=0.004)	Mann Whitney U	U = 36.0	0.005	δ = 1.00 (very large)

To minimize the confounding influence of technical artifacts and non-contractile tissues, a focused comparison was conducted using only the highest-quality strip from each animal. Analysis of the rhythmic phase AUC in this subset revealed a striking group separation: every selected control strip exhibited substantially greater contractile activity than all IDA strips.

A Mann–Whitney U test confirmed this separation was statistically significant ($U = 36.0$, $p = 0.0022$). This U value represents the maximum possible rank separation for groups of equal size ($n_1 = n_2 = 6$), indicating complete non-overlap between control and IDA values.

The corresponding effect size, Cliff's $\delta = 1.00$, reflects absolute stochastic dominance of the control group—a rare and robust finding.

As an additional validation, an independent t-test was performed on log-transformed AUC values to account for skewness. This also revealed a highly significant group difference (Welch's $t(\approx 5.9) = 5.91$, $p = 0.002$). The calculated Hedges' $g \approx 3.1$ indicates a very large effect size, suggesting that the mean contractile output in control samples was approximately three standard deviations higher than that of IDA samples.

Chapter 4 illustrates this disparity: while baseline AUC values were comparably low in both groups (consistent with quiescent tone), rhythmic phase AUC values in control strips were orders of magnitude higher, reflecting robust, sustained spontaneous contractions. By contrast, even the most responsive IDA strips produced minimal force-time area, consistent with a marked impairment in phasic contractility.

5.12. Results Overview

This thesis sets out to determine how maternal IDA affects uterine contractile function in late pregnancy. Using an experimental Sprague-Dawley rat model, the research examined whether a diet-induced iron deficiency alters the baseline passive tension and spontaneous contraction patterns of the myometrium. The study's methodology involved ex vivo organ bath recordings of isolated uterine muscle strips from late-gestation IDA-treated dams versus controls, allowing precise measurement of contractile indices. The central hypothesis was that an IDA diet would lead to a lower resting uterine tone and potentially trigger earlier or more frequent spontaneous contractions than a normal iron-sufficient diet, thereby increasing the risk of a transition into labor-like activity (and by extension, a predisposition to premature labor). All procedures were conducted with careful controls to isolate the effect of iron deficiency on uterine muscle behavior. In summary, the objective, through this method, was to directly test if iron deficiency compromises myometrial contractility as hypothesized.

5.13. Research Contributions

This study found clear evidence that maternal IDA profoundly impacts uterine contractility, yielding several key findings. First, uterine strips from IDA-diet rats showed a

markedly lower baseline passive tension compared to those from iron-sufficient control rats, indicating reduced inherent uterine muscle tone. Second, the IDA myometrium failed to develop the robust spontaneous contractions observed in controls during late pregnancy. While control samples exhibited strong, rhythmic contractions (with significant peak forces and integrated tension over time), the IDA samples often remained largely quiescent or only produced very weak, uncoordinated twitches. In fact, any spontaneous contractions in the IDA group were of significantly smaller amplitude and the overall contractile work (quantified by the area under the tension–time curve) was only a fraction of that in the control group. These results confirm that iron deficiency directly affects myometrial function by diminishing both the strength and regularity of uterine contractions. The findings contribute to scientific knowledge by providing direct experimental evidence linking iron availability to uterine muscle performance. This thesis's contribution is twofold: it quantitatively demonstrates how IDA leads to uterine hypo-contractility (a potential mechanism for labor dysfunction), and it highlights the importance of maternal nutritional status (iron levels) as a factor in pregnancy outcomes. By elucidating this relationship, the research fills a gap in the literature on the myometrial effects of iron deficiency, offering insight into why IDA is clinically associated with higher risks of preterm labor and uterine atony.

5.14. Discussion of Limitations

When interpreting these results, it is important to consider the reliability and limitations of the data and analysis undertaken. This research employed a controlled experimental setup and validated instruments; however, certain constraints should be acknowledged. The sample size for the IDA group was relatively small (due in part to the challenges of inducing and maintaining iron deficiency in pregnant dams), which may limit the statistical power of some comparisons. Despite this, the differences observed were consistently large – especially in the most reliable data segments – suggesting that the effects of IDA on uterine contractility are real and not an artifact of random variation. The study took steps to ensure data quality, such as excluding recordings from malfunctioning transducer channels and averaging metrics per animal to treat the dam as the unit of analysis.

Even so, a few recordings in the IDA group had to be discarded due to technical issues (e.g., noise or loss of tension signal), resulting in a conservative analysis focused on high-quality data. This cautious curation of data improves confidence in the findings but also

underscores a limitation: some degree of selection was necessary, which could introduce bias if, for instance, the most severe IDA cases were also the ones with unusable data. Furthermore, the use of an ex vivo organ bath system, while allowing precise control over conditions, means the results reflect an isolated tissue response. In a living animal (or human), systemic factors such as hormonal environment, blood flow, and neural inputs also influence uterine contractility. The discussion in this thesis addressed these issues by comparing the experimental conditions to *ex vivo* physiology and by consulting existing literature – lending context that the observed phenomenon (reduced contractility in IDA) is biologically plausible given iron's role in muscle function. Overall, the reliability of the results is supported by the strong signal observed (large differences between groups) and alignment with known muscle physiology, but the above limitations should be kept in mind when generalizing these findings.

5.15. Implications and Suggestions for Future Research

The outcomes of this study are expected to carry implications for both clinical practice and future research. From a clinical perspective, the clear association between iron deficiency and diminished uterine contractile performance suggests that pregnant individuals with IDA may be at greater risk for labor abnormalities, such as weak contractions or even failure to progress in labor. Therefore, one practical recommendation is to enhance screening and early intervention for IDA during pregnancy. Ensuring adequate iron intake or providing iron supplementation when deficiency is identified could be vital not just for preventing anemia-related fatigue or fetal developmental issues, but also for securing proper uterine function at the time of delivery. Obstetric management protocols might incorporate the findings by more closely monitoring uterine activity in anemic patients and being prepared for potential uterine atony or other labor dysfunctions. From a research standpoint, this thesis opens several avenues for further investigation. A logical next step would be to explore the cellular and molecular mechanisms underlying the observed contractile deficits in IDA uteri – for instance, examining whether iron deficiency alters calcium handling in myometrial cells, impairs ATP production in uterine muscle fibers, or modulates the expression of ion channels and gap junctions that are crucial for coordinated contractions. Future studies could also address the timeline of these changes: at what stage of iron deficiency do myometrial alterations become significant, and are they reversible with

iron repletion? Another suggestion is to extend this research to *ex vivo* models or clinical studies. For example, investigators could measure uterine activity (using techniques like electromyography or pressure catheters) in iron-deficient versus iron-replete pregnant subjects to confirm that the ex vivo findings translate to actual differences in contraction patterns during labor. Such studies would further validate the clinical relevance of the present findings. Additionally, testing therapeutic interventions in the rat model – such as whether administering iron therapy to IDA-affected dams late in pregnancy can restore normal uterine contractility – would directly assess the potential to mitigate the risks identified. Overall, the implications underscore that maternal nutrition has a direct effect on the biomechanics of childbirth, and future research should continue to integrate nutritional status into the understanding of parturition physiology.

5.16. Conclusion

In conclusion, this thesis has demonstrated that iron deficiency anemia in pregnancy is not only a hematological concern but also a condition with significant biomechanical consequences for the uterus. The research objective of determining the effect of an IDA diet on rat uterine contractile function was successfully addressed through carefully designed experiments, and the central hypothesis was investigated in depth. The key discovery is that an iron-poor diet leads to a measurable weakening of the myometrium's intrinsic tone and contractile capacity, offering a physiological explanation for the clinically observed link between maternal anemia and adverse labor outcomes. By establishing this link, the study contributes new insight to the field of reproductive physiology and obstetrics: it identifies uterine smooth muscle as a target of iron deficiency, thereby broadening the understanding of how maternal health translates into labor performance. The findings also reinforce the importance of holistic prenatal care – confirming that adequate nutritional status, particularly iron sufficiency, is crucial for the normal function of the uterus as much as for the oxygen-carrying capacity of blood. While there are limitations to consider (such as sample size and experimental scope, as discussed), the evidence presented is compelling and builds a strong case that improving iron status in expecting mothers could have direct benefits in terms of reducing the risk of labor complications. In summary, this research underscores that addressing IDA in pregnancy is important not only for preventing anemia-related symptoms and fetal development issues, but also for ensuring that the uterus is physiologically prepared

for the demands of labor. The hope is that these insights will pave the way for further studies and ultimately inform clinical strategies to improve maternal and neonatal outcomes.

6. REFERENCES

1. Malik MT, Malik RT, Tariq A (2023). Iron Deficiency Anaemia: The Psychological Menace. JPMA The Journal of the Pakistan Medical Association 73: 1568.
2. Banerjee A, Athalye S, Shingade P, Khargekar V, Mahajan N, Madkaikar M, Khargekar N (2024). Efficacy of daily versus intermittent oral iron supplementation for prevention of anaemia among pregnant women: a systematic review and meta-analysis. eClinicalMedicine 74.
3. Nicholson WK, Silverstein M, Wong JB, Chelmow D, Coker TR, Davis EM, Jaén CR, Krousel-Wood M, Lee S, Li L, Rao G, Ruiz JM, Stevermer J, Tsevat J, Underwood SM, Wiehe S (2024). Screening and Supplementation for Iron Deficiency and Iron Deficiency Anemia During Pregnancy: US Preventive Services Task Force Recommendation Statement. JAMA 332: 906–913.
4. Pratima Verma, Anuradha Roy (2024). Iron Deficiency Anemia (IDA) in Pregnancy : Prevalence and Management. Ayushdhara 257–261.
5. McLean E, Cogswell M, Egli I, Wojdyla D, De Benoist B (2009). Worldwide prevalence of anaemia, WHO Vitamin and Mineral Nutrition Information System, 1993-2005. Public Health Nutrition 12: 444–454.
6. Merdin A (2019). Evaluation Of Iron Deficiency Anemia Awareness In a Rural Area: Results From a Survey In a Mediterranean Region Rural Area Of Turkey. Acta Oncologica Turcica 52: 132–135.
7. DeLoughery EP (2024). Global prevalence of anemia among women of reproductive age, 2000–2019. European Journal of Haematology 113: 253–256.
8. Gardner W, Kassebaum N (2020). Global, Regional, and National Prevalence of Anemia and Its Causes in 204 Countries and Territories, 1990–2019. Current Developments in Nutrition 4: 830.
9. Hasan MM, Soares Magalhaes RJ, Garnett SP, Fatima Y, Tariqujjaman M, Pervin S, Ahmed S, Mamun AA (2022). Anaemia in women of reproductive age in low- and middle-income countries: progress towards the 2025 global nutrition target. Bulletin of the World Health Organization 100: 196–204.

10. Thorat S, Walton JR, Lindahl PA (2023). A kinetic model of iron trafficking in growing Saccharomyces cerevisiae cells; applying mathematical methods to minimize the problem of sparse data and generate viable autoregulatory mechanisms. PLoS Computational Biology 19.

11. Abioye AA, Owopetu CA, Adamu-Adedipe, Foyekemi Oyebola, Odesanya LO, Olofin-Samuel MA (2024). Anaemia Prevention Among Pregnant Women.

12. Pavord S, Myers B, Robinson S, Allard S, Strong J, Oppenheimer C (2012). UK guidelines on the management of iron deficiency in pregnancy. British Journal of Haematology 156: 588–600.

13. Breymann C (2015). Iron Deficiency Anemia in Pregnancy. Seminars in Hematology 52: 339–347.

14. Scholl TO (2011). Maternal iron status: relation to fetal growth, length of gestation, and iron endowment of the neonate. Nutrition Reviews 69 Suppl 1.

15. Zimmermann MB, Hurrell RF (2007). Nutritional iron deficiency. The Lancet 370: 511–520.

16. Bencaiova G, Burkhardt T, Breymann C (2012). Anemia—prevalence and risk factors in pregnancy. European Journal of Internal Medicine 23: 529–533.

17. Reveiz L, Gyte GM, Cuervo LG (2007). Treatments for iron-deficiency anaemia in pregnancy. In: Reveiz L, editor. *Cochrane Database of Systematic Reviews* Chichester, UK: John Wiley & Sons, Ltd. doi:10.1002/14651858.CD003094.pub2.

18. Wachs TD, Georgieff M, Cusick S, McEwen BS (2014). Issues in the timing of integrated early interventions: contributions from nutrition, neuroscience, and psychological research. Annals of the New York Academy of Sciences 1308: 89–106.

19. Solovyeva A V., Ermolenko KS, Kulumbegova LT, Aleynikova EYu, Chegus LA (2023). Replenishment of iron deficiency in women before the use of assisted reproductive technologies. Meditsinskiy sovet = Medical Council 53–56. doi:10.21518/ms2023-324.

20. Wang R, Xu S, Hao X, Jin X, Pan D, Xia H, Liao W, Yang L, Wang S (2025). Anemia during pregnancy and adverse pregnancy outcomes: a systematic review and meta-analysis of cohort studies. Frontiers in Global Women's Health 6.

21. Ali M, Mugheri IA, Abro NN, Sangi SUN, Bhatti AT, Shiakh S (2024). Serum Ferritin Level and Total Iron Binding Capacity Relationship with Iron Deficiency Anemia During Pregnancy and Labour. Journal of Health and Rehabilitation Research 4: 1234–1238.

22. Simsek Z, Atalay B, Keklik AZ, Akbaba M, Ertem M (2018). Epidemiology of Micronutrient Deficiencies in Agricultural Reproductive-Aged Female Workers in Southeastern Anatolia, Turkey. The Turkish Journal Of Occupational Environmental Medicine and Safety 3: 9–9.

23. Yaylacı F, Özek Erkuran H, Çetin FH, Kara H (2019). Dikkat Eksikliği Hiperaktivite Bozukluğu Tedavisinde Neurofeedback Eğitimi. Psikiyatride Guncel Yaklasimlar - Current Approaches in Psychiatry 11: 531–546.

24. Kara B, Çal S, Aydoğan A, Sarper N (2006). The Prevalence of Anemia in Adolescents. Journal of Pediatric Hematology/Oncology 28: 316–321.

25. Simsek Z, Atalay B, Keklik AZ, Akbaba M, Ertem M (2018). Epidemiology of micronutrient deficiencies in agricultural reproductive-aged female workers in Southeastern Anatolia, Turkey. The Turkish Journal of Occupational / Environmental Medicine and Safety 3(1): 1-9.

26. Tosyali M, Koç F (2024). Adherence to iron supplementation during the first year of life infants in Izmir, Turkey. Medicine (United States) 103: e38926.

27. Zangeneh FZ, Hantoushzadeh S (2023). The physiological basis with uterine myometrium contractions from electro-mechanical/hormonal myofibril function to the term and preterm labor. Heliyon 9.

28. Tsymbalyuk O V., Vadzyuk OB, Voiteshenko IS, Ivanova VD (2022). Participation of KATP-channels of plasma and mitochondrial membranes in the regulation of mechanokinetics of rat myometrium spontaneous contractions. Studia Biologica 16: 19–34.

29. Ferreira JJ, Amazu C, Puga-Molina LC, Ma X, England SK, Santi CM (2021). SLO2.1/NALCN a sodium signaling complex that regulates uterine activity. iScience 24: 103210.

30. Wray S, Arrowsmith S (2021). Uterine Excitability and Ion Channels and Their Changes with Gestation and Hormonal Environment. Annual Review of Physiology 83: 331–357.

31. Anghileri LJ, Thouvenot P (1998). ATP in iron overload-induced intracellular calcium changes. International Journal of Molecular Medicine 1(5): 869-873.

32. Vinke JSJ, Gorter AR, Eisenga MF, Dam WA, van der Meer P, van den Born J, Bakker SJL, Hoes MF, de Borst MH (2023). Iron deficiency is related to lower muscle mass in community-dwelling individuals and impairs myoblast proliferation. Journal of Cachexia, Sarcopenia and Muscle 14: 1865–1879.

33. Halilzade Mİ, Halilzade İ, Kokanalı MK (2024). A new effect of intravenous iron treatment in pregnancy: contraction in nonstress test and timing of labor. Revista da Associação Médica Brasileira 70.

34. Frise MC, Holdsworth DA, Johnson AW, Chung YJ, Curtis MK, Cox PJ, Clarke K, Tyler DJ, Roberts DJ, Ratcliffe PJ, *et al.* (2022). Abnormal whole-body energy metabolism in iron-deficient humans despite preserved skeletal muscle oxidative phosphorylation. Scientific Reports 12: 998.

35. Sungkar T, Rozi MF, Dairi LB, Zain LH (2019). Serum Ferritin Levels: A Potential Biomarker to Represent Child-Turcotte-Pugh Score among Decompensated Liver Cirrhosis Patients. Malaysian Journal of Medical Sciences 26: 59–65.

36. Watkins VY, Frolova AI, Stout MJ, Carter EB, Macones GA, Cahill AG, Raghuraman N (2020). The relationship between maternal anemia and umbilical cord oxygen content at delivery. American Journal of Obstetrics & Gynecology *MFM* 3: 100270.

37. Kato H, Kuwatsuru R (2018). Anatomy of Uterine Blood Supply and the Prevention of Massive Hemorrhage. Gynecologic and Obstetric Prophylactic Hemostasis by Intra-arterial Balloon Occlusion Singapore: Springer Singapore, pp 1–6. doi:10.1007/978-981-10-8833-9_1.

38. Cicinelli E (2004). Blood to the cornual area of the uterus is mainly supplied from the ovarian artery in the follicular phase and from the uterine artery in the luteal phase. Human Reproduction 19: 1003–1008.

39. Girling JC (2004). Physiology of pregnancy. Anaesthesia & Intensive Care Medicine 5: 215–218.

40. Moore LG, Wesolowski SR, Lorca RA, Murray AJ, Julian CG (2022). Why is human uterine artery blood flow during pregnancy so high? American Journal of Physiology-Regulatory, Integrative and Comparative Physiology 323: R694–R699.

41. Osikoya O, Hula N, da Silva R de NO, Goulopoulou S (2024). Perivascular Adipose Tissue and Uterine Artery Adaptations to Pregnancy. Microcirculation 31: e12857.

42. Aujla T, Darby JRT, Saini BS, Lock MC, Holman SL, Bradshaw EL, Perumal SR, McInnes SJP, Voelcker NH, Wiese MD, Macgowan CK, Seed M, Morrison JL (2021). Impact of resveratrol-mediated increase in uterine artery blood flow on fetal haemodynamics, blood pressure and oxygenation in sheep. Experimental Physiology 106: 1166–1180.

43. Maybin JA (2021). Hypoxia and reproductive health. Reproduction 161: E1–E2.

44. Ng KYB, Mingels R, Morgan H, Macklon N, Cheong Y (2018). In vivo oxygen, temperature and pH dynamics in the female reproductive tract and their importance in human conception: a systematic review. Human Reproduction Update 24: 15–34.

45. Wray S, Alruwaili M, Prendergast C (2021). Hypoxia and labour. 161(1): F67-F80.

46. Wang Z, Camm EJ, Nuzzo AM, Spiroski AM, Skeffington KL, Ashmore TJ, Rolfo A, Todros T, Logan A, Ma J, Murphy MP, Niu Y, Giussani DA (2024). *In vivo* mitochondria-targeted protection against uterine artery vascular dysfunction and remodelling in rodent hypoxic pregnancy. The Journal of Physiology 602: 1211–1225.

47. Peebles DM, Edwards AD, Wyatt JS, Cope M, Delpy DT, Osmund E, Reynold R (1992). Changes in human fetal cerebral oxygenation and blood volume during delivery. American Journal of Obstetrics and Gynecology 167: 1916–1917.

48. Mollard P, Mironneau J, Amedee T, Mironneau C (1986). Electrophysiological characterization of single pregnant rat myometrial cells in short-term primary culture. American Journal of Physiology-Cell Physiology 250: C47–C54.

49. Wray S, Taggart MJ (2024). An update on pacemaking in the myometrium. J Physiol doi: 10.1113/JP284753, Online ahead of print.

50. Cahill AG, Wen Z, Wang H, Zhao P, Sun Z, Schwartz AL, Wang Y (2022). Analysis of Electrophysiological Activation of the Uterus During Human Labor Contractions. JAMA Network Open 5: e2214707.

51. Garrett AS, Roesler MW, Athavale ON, Du P, Clark AR, Cheng LK (2022). In vivo multi-channel measurement of electrical activity of the non-pregnant rat uterus. 2022 44th Annual International Conference of the IEEE Engineering in Medicine & Biology Society (EMBC) IEEE, pp 3682–3685. doi:10.1109/EMBC48229.2022.9871943.

52. Arrowsmith S, Wray S (2014). Oxytocin: Its Mechanism of Action and Receptor Signalling in the Myometrium. Journal of Neuroendocrinology 26: 356–369.

53. Young RC (2007). Myocytes, myometrium, and uterine contractions. Annals of the New York Academy of Sciences 1101: 72–84.

54. Smith R (2007). Parturition. New England Journal of Medicine 356: 271–283.

55. Mudrov VA, Андреевич MB (2022). Modern concepts about the mechanisms of initiation and regulation of labor activity. Journal of Obstetrics and Women's Diseases 71: 87–100.

56. Hamburg-Shields E, Mesiano S (2024). The hormonal control of parturition. Physiological Reviews 104: 1121–1145.

57. Caine M, Monaghan S, Macnab WR (2022). Uterine physiology. *Anaesthesia and* Intensive Care Medicine 23: 341–343.

58. Reinl EL, England SK (2015). Fetal-to-maternal signaling to initiate parturition. Journal of Clinical Investigation 125: 2569–2571.

59. Khader N, Dorogin A, Shynlova O, Mitchell JA (2025). JUND plays a genome-wide role in the quiescent to contractile switch in the pregnant human myometrium. PLoS Genet 21(6): e1011261.

60. Enazy SA, Kirschen GW, Vincent K, Yang J, Saada J, Shah M, Oberhauser AF, Bujalowski PJ, Motamedi M, Salama SA, Kilic G, Rytting E, Borahay MA (2023). PEGylated Polymeric Nanoparticles Loaded with 2-Methoxyestradiol for the Treatment of Uterine Leiomyoma in a Patient-Derived Xenograft Mouse Model. Journal of Pharmaceutical Sciences 112: 2552–2560.

61. Alqarni AM, Alghamdi AA, Aljubran HJ, Bamalan OA, Abuzaid AH, Alyahya MA, Alawami AM, Al Shubbar MD, Al Yousif GF (2024). Exploring the Impact of Iron Deficiency Anaemia on Glycated Haemoglobin A1c Levels in Pregnant and Non-Pregnant Women: A Systematic Review. International Journal of Women's Health 16: 797.

62. Omotayo MO, Abioye AI, Kuyebi M, Eke AC (2021). Prenatal anemia and postpartum hemorrhage risk: A systematic review and meta-analysis. Journal of Obstetrics and Gynaecology Research 47: 2565–2576.

63. Muir R, Ballan J, Clifford B, McMullen S, Khan R, Shmygol A, Quenby S, Elmes M (2016). Modelling maternal obesity: the effects of a chronic high-fat, high-cholesterol diet on uterine expression of contractile-associated proteins and *ex vivo* contractile activity during labour in the rat. Clinical Science 130: 183–192.

64. Rizwan Ahmad AM, Farooq U, Anees M, Anis RA, Rashid S, Ahmed W (2022). Co-administration of Inulin and Iron Fortificants improves Iron Deficiency Biomarkers in Female Sprague Dawley Rats. Food Science and Nutrition 10: 2141–2148.

65. Chang Y-H, Chen W-H, Su C-H, Yu H-R, Tain Y-L, Huang L-T, Sheen J-M (2022). Maternal Iron Deficiency Programs Rat Offspring Hypertension in Relation to Renin—Angiotensin System and Oxidative Stress. International Journal of Molecular Sciences 23: 8294.

66. Ameer MA, Fagan SE, Sosa-Stanley JN, Peterson DC (2019, July 11). Anatomy, Abdomen and Pelvis, Uterus.

67. Kelsey TW, Ginbey E, Chowdhury MM, Bath LE, Anderson RA, Wallace WHB (2016). A Validated Normative Model for Human Uterine Volume from Birth to Age 40 Years. PLOS ONE 11: e0157375.

68. Li J, Wang Y, Tang R, Peng Y, Wang Y, Liu B, Jiang Y, Liu G, Lin S, Chen R (2020). Changes in ultrasound uterine morphology and endometrial thickness during ovarian aging and possible associated factors: findings from a prospective study. Menopause 27: 794–800.

69. Anatomy of the Female Reproductive System | Lecturio (n.d.). Available at: https://app.lecturio.com/#/course/s/86877/?return=/search/courses/uterus. [Accessed: 31 October 2024].

70. Ellis H (2011). Anatomy of the uterus. Anaesthesia and Intensive Care Medicine 12: 99–101.

71. Ameer MA, Fagan SE, Sosa-Stanley JN, Peterson DC (2022). Anatomy, Abdomen and Pelvis: Uterus. StatPearls.

72. Kagami K, Ono M, Iizuka T, Matsumoto T, Hosono T, Sekizuka-Kagami N, Shinmyo Y, Kawasaki H, Fujiwara H (2020). A novel third mesh-like myometrial layer connects the longitudinal and circular muscle fibers -A potential stratum to coordinate uterine contractions-. Scientific Reports *2020 10:1* 10: 1–7.

73. Menon R, Bonney EA, Condon J, Mesiano S, Taylor RN (2016). Novel concepts on pregnancy clocks and alarms: redundancy and synergy in human parturition. Human Reproduction Update 22: 535–560.

74. Escalante M NM, Henríquez Pino J (2017). Arrangement of muscle fibers in the myometrium of the human uterus: a mesoscopic study. MOJ Anatomy & Physiology Volume 4.

75. Jain V, Saade GR, Garfield RE (2000). Structure and function of the myometrium. Advances in Organ Biology 8: 215–246.

76. Bulletti C, De Ziegler D, Setti PL, Cicinelli E, Polli V, Stefanetti M (2004). Myomas, pregnancy outcome, and in vitro fertilization. Annals of the New York Academy of Sciences 1034: 84–92.

77. Wray S, Prendergast C (2019). The Myometrium: From Excitation to Contractions and Labour. Advances in Experimental Medicine and Biology 1124: 233–263.

78. Garfield RE, Murphy L, Gray K, Towe B (n.d.). Review and Study of Uterine Bioelectrical Waveforms and Vector Analysis to Identify Electrical and Mechanosensitive Transduction Control Mechanisms During Labor in Pregnant Patients. doi:10.1007/s43032-020-00358-5/Published.

79. Jones K, Shmygol A, Kupittayanant S, Wray S (2004). Electrophysiological characterization and functional importance of calcium-activated chloride channel in rat uterine myocytes. Pflugers Archiv European Journal of Physiology 448: 36–43.

80. Shynlova O, Nadeem L, Lye S (2023). Progesterone control of myometrial contractility. The Journal of Steroid Biochemistry and Molecular Biology 234: 106397.

81. Benson AE, Shatzel JJ, Ryan KS, Hedges MA, Martens K, Aslan JE, Lo JO (2022). The incidence, complications, and treatment of iron deficiency in pregnancy. *European* Journal of Haematology 109: 633–642.

82. Lee JK, He Y, Flores SR, Woloshun RR, Wang X, Shine JS, Ebea-Ugwuanyi PO, Sriram S, Fraga M, Zhu S, Yu Y, Hamza I, Collins JF (2025). Development of rat and mouse models of heme-iron absorption. JCI Insight 10(11): e184742.

83. Arrowsmith S, Keov P, Muttenthaler M, Gruber CW (2018). Contractility Measurements of Human Uterine Smooth Muscle to Aid Drug Development. Journal of Visualized Experiments 131: 56639.

84. He H, Huang Q, Liu C, Jia S, Wang Y, An F, Song H (2019). Effectiveness of AOS–iron on iron deficiency anemia in rats. RSC Advances 9: 5053–5063.

85. Chung YJ, Luo A, Park KC, Loonat AA, Lakhal-Littleton S, Robbins PA, Swietach P (2019). Iron-deficiency anemia reduces cardiac contraction by downregulating RyR2 channels and suppressing SERCA pump activity. JCI Insight 4(7): e125618..

86. Frass KA (2015). Postpartum hemorrhage is related to the hemoglobin levels at labor: Observational study. Alexandria Journal of Medicine 51: 333–337.

87. LaBorde JB, Wall KS, Bolon B, Kumpe TS, Patton R, Zheng Q, Kodell R, Young JF (1999). Haematology and serum chemistry parameters of the pregnant rat. Laboratory Animals 33: 275–287.

88. Gáspár R, Hajagos-Tóth J, Schaffer A, Kothencz A, Siska-Szabó L, Ducza E, Csányi A, Tábi T, Bagaméry F, Szökő É, Kovács O, Barna T, Samavati R, Mirdamadi M, Sztojkov-Ivanov A, Szűcs KF, Vari SG (2022). High Fat High Sucrose Diet Modifies Uterine Contractility and Cervical Resistance in Pregnant Rats: The Roles of Sex Hormones, Adipokines and Cytokines. *L*ife 12: 794.

89. Sondgeroth K, Boyman E, Pathare R, Porta M (2025). Voltage-Gated Calcium Channels and the Parity-Dependent Differential Uterine Response to Oxytocin in Rats. Reproductive Sciences 32: 300–315.

90. Joyce EM, Diaz P, Tamarkin S, Moore R, Strohl A, Stetzer B, Kumar D, Sacks MS, Moore JJ (2016). In-vivo stretch of term human fetal membranes. Placenta 38: 57–66.

91. Rao R, Tkac I, Unger EL, Ennis K, Hurst A, Schallert T, Connor J, Felt B, Georgieff MK (2013). Iron supplementation dose for perinatal iron deficiency differentially alters the neurochemistry of the frontal cortex and hippocampus in adult rats. Pediatric Research 73: 31–37.

92. Chen X, Han C, Zhao JP, Shen S, Wang LY, Ren S, Wang TL, Ma Y, Xu ZC, Huo JS (2024). Establishment of an Iron Deficiency Model by Iron Depletion in Pregnant Rats. Biomedical and Environmental Sciences 37: 210–215.

93. Nilüfer Akgün Ünal, Fatma Sare Taştepe (2021). The effects of maternal zinc deficiency on myometrial contractility: an in vitro study. Kastamonu Medical Journal 71–74. doi:10.51271/KMJ-0017.

94. Wray S, Prendergast C (2019). The Myometrium: From Excitation to Contractions and Labour pp 233–263. doi:10.1007/978-981-13-5895-1_10.

95. Woodman AG, Care AS, Mansour Y, Cherak SJ, Panahi S, Gragasin FS, Bourque SL (2017). Modest and Severe Maternal Iron Deficiency in Pregnancy are Associated with Fetal Anaemia and Organ-Specific Hypoxia in Rats. Scientific Reports 7: 46573.

96. Hossain MR, Paul M, Tolosa JM, Smith R, Paul JW (2025). Assessing Tocolytic Potency: Variability and Accuracy of AUC Versus Amplitude-Based Assessment of Pregnant Human Myometrial Contractions Ex Vivo. Reproductive Sciences 32: 2027–2049.

APPENDICES

CURRICULUM VITAE

PERSONAL INFORMATION		
Name	Mahindokht Rouhikia	
Nationality	Iranian	
Date of Birth		
Phone:		
E-mail:		
Educational Background		
Degree	**Name of Institution**	**Year of Graduation**
Master's degree	University of Social Welfare and Rehabilitation Sciences, Tehran- Iran	2008
Bachler	Iran University of Medical Science (IUMS)	2003
High School	Sherafat High School- Tehran- Iran	1986
Languages:		
1. Turkish	Work Proficiency	
2. English	Work Proficiency	
3. Farsi	Native	
4. Arabic	Intermediate	
5. Russian	Beginner	
6. Germani	Beginner	

AREA OF EXPERTISE	
1. QEEG	
2. ERP	
3. Biofeedback Training	
4. Neurotherapy	
5. Peak Performance Training	
6. Cognitive Training	
7. Joint Mobilization Technique	
PUBLICATIONS (Must be written according to thesis writing rules)	
1	Yazar U, Guvercin AR, Rouhikia M, Aktoklu M, Demirci MA, Erbay I, Ayar A (2023). Cerebrolysin provides effective protection on high glucose-induced neuropathy in cultured rat dorsal root ganglion neurons. Journal of Receptors and Signal Transduction 43: 109–114.]
DECLARATIONS	
1	2019, Preventive Medicine and Telemedicine. 10th Edition of International Conference on Preventive Medicine & Public Health. https://preventivemedicine.euroscicon.com/2019/renowned-speakers
2	2017, Clinical use of QEEG (functional brain mapping) in rehabilitation. Proceedings of the 5th International Conference on Physiotherapy (Dubai,

	UAE)- https://www.omicsonline.org/proceedings/clinical-use-of-qeeg-functional-brain-mapping-in-rehabilitation-92209.html
3.	2016, Biofeedback treatment in sport rehabilitation. Proceedings of the 2nd International Conference on Sports Medicine and Fitness (Dubai, UAE). https://www.hilarispublisher.com/proceedings/biofeedback-treatment-in-sport-rehabilitation-4958.html
Awards / Incentives / Scholarships	
1.	**Scientific Research Project (BAP) Incentive**, [KTÜ], ₺40,000, [2023]
2.	
3.	
HOBİLER	
1.	Language Learning
2.	Music & Movies
3.	Reading
4.	Swimming